ISSN 1028-8546

Volume XXIII, Number 4
Section: En
December, 2017

Azerbaijan Journal of Physics

Fizika

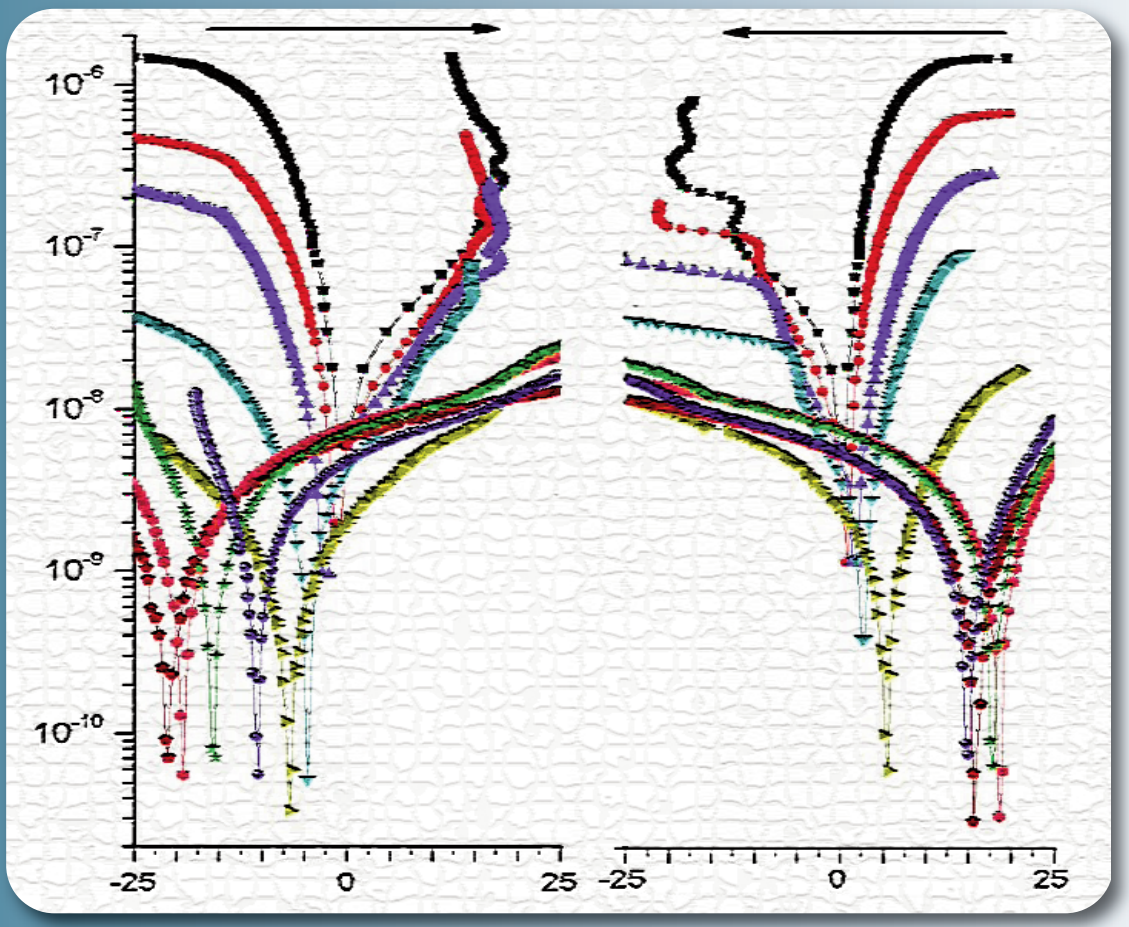

www.physics.gov.az

G.M. Abdullayev Institute of Physics
Azerbaijan National Academy of Sciences
Department of Physical, Mathematical and Technical Sciences

Published from 1995
Ministry of Press and Information
of Azerbaijan Republic,
Registration number 402, 16.04.1997

ISSN 1028-8546
vol. XXIII, Number 04, 2017
Series: En

Azerbaijan Journal of Physics

FIZIKA

G.M.Abdullayev Institute of Physics
Azerbaijan National Academy of Sciences
Department of Physical, Mathematical and Technical Sciences

PUBLISHING OFFICE

131 H.Javid ave, AZ-1143, Baku
ANAS, G.M.Abdullayev Institute of Physics

Tel.: (99412) 538-76-46, 539-32-23
Fax: (99412) 537-22-92
E-mail: jophphysics@gmail.com
Internet: www.physics.gov.az

It is authorized for printing:

Published at "**SƏRQ-QƏRB**"
17 Ashug Alessger str., Baku
Typographer : Aziz Gulaliyev

Sent for printing on: __.__. 201_
Printing approved on: __.__. 201_
Physical binding:_____
Number of copies:_____200
Order:_____

MODELLING OF MOLTEN ZONE LENGTH INFLUENCE ON COMPONENT CONCENTRATION DISTRIBUTION IN InAs-GaAs CRYSTALS GROWN BY MODIFIED ZONE MELTING METHOD

Z.M. ZAKHRABEKOVA, A.I. ALEKPEROV, G.H. AJDAROV
Institute of Physics of Azerbaijan NAS, AZ-1143, Baku, H.Javid ave.,33, Baku-143
E-mail: zangi@physics.ab.az, тел.:(+99412)5393218, Fax: (+99412)4395961

The task of component concentration distribution along Ge-Si solid solution crystals grown by modified zone melting method using the InAs-seed crystal is solved in the fully mixed melt approximation.

The component axial concentration profiles in crystals grown at different molten zone lengths are calculated taking under consideration the complicated dependence of GaAs segregation coefficient on the melt composition. The possibility of control by component concentration distribution in wide range in InAs-GaAs crystals by the way of molten zone length changes is shown. The analysis of obtained results defines the optimal technological parameters for growing of solid InAs-GaAs solution crystals with given homogeneous and alternative compositions along the matrix.

Keywords: InAs, GaAs, solid solutions, Phann approximation, molten zone, component distribution.
PACS: 81.10.Aj

INTRODUCTION

The obtaining of material with given concentration component distribution in matrix and support of its monocrystallinity is the main technological problem of volume crystal growing of semiconductor solid solutions from the melt.

InAs-GaAs system the composite components of which are the basic materials of modern micro-and opto-electronic industry, presents the special interest in the set of semiconductor solid solutions. In and GaAs fully dissolve in each other in any ratios in both liquid and solid states and form the continuous set of exchange solid solutions [1].

The math modeling of component concentration profile along InAs-GaAs crystals grown by modified zone recrystallization method using InAs-seed crystal is carried out in the given work in Phann approximation. The aim is potential establishing of modified method for obtaining of InAs-GaAs volume single crystals with given component axial concentration distribution. Note that the tasks on modeling of component concentration profiles are solved earlier for Ge-Si crystals grown from the melt by the series of conservative and non-conservative methods [3-10]. The results of these works show the well coincidence with experimental data.

RESULTS AND DISCUSSIONS

The conceptual scheme of solid solution crystal growing by modified method of zone melting is presented in fig.1. The single-crystal seed (1) from InAs (fig.1A) is put into crucible of cylinder form. The previously prepared rods of definite diameter from InAs (2) and macro-homogeneous solid solution InAs-GaAs with given composition (3) are put under seed. The rod melting (2) from InAs put directly under seed (fig.1B) is carried out in vacuum conditions. The temperature in melt boundaries with seed and ingot in prestarting moment of recrystallization is equal to melting point of InAs. The crystal growth takes place in seed from the moment of switching of crucible-moving mechanism relatively to heater and continues up to ingot total recrystallization (3). The length of final molten zone is supported as constant and equal to Z up to moment of its formation. Here the final molten zone consists in pure InAs as opposed to traditional zone melting method [2,11]. This circumstance solves the problem of seed which is necessary for growing of single crystals of Ge-Si solid solutions of different compositions by the way of using the InAs-seed.

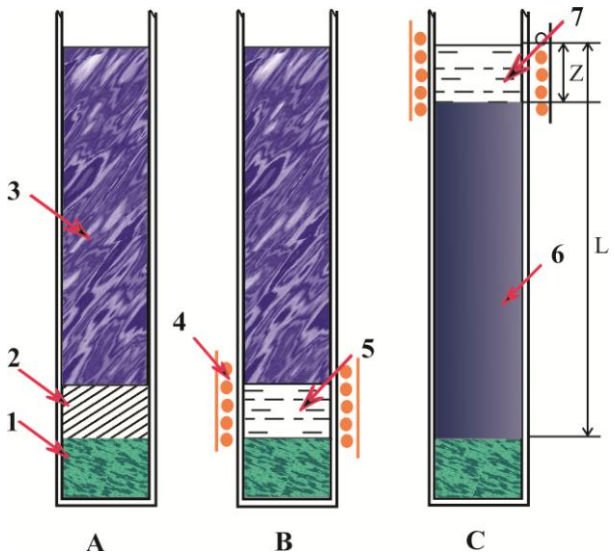

Fig.1. Growing circuit of single crystal InAs-GaAs solid solutions by modified zone melting method using the InAs-seed. A is order of crucible loading: 1 and 2 are seeding and rod from InS, 3 is macro-homogeneous rod from InAs-GaAs of given composition, C is moment of final molten zone formation; B is crystallization starting point: 4 is heater, 5 is melt from InAs, C is moment of final molten zone formation: 6 is InAs-GaAs single crystal, 7 is InAs-GaAs meltl L and Z are lengths of given regions.

The task of concentration distribution of InAs and GaAs along InAs-GaAs crystal grown by modified zone melting method is solved in Phann approximation at

131 H.Javid ave, AZ-1143, Baku
ANAS, G.M.Abdullayev Institute of Physics
E-mail: jophphysics@gmail.com

carrying out of following standard conditions [11]: component diffusion in solid phase is negligible quantity; crystallization front is plane; there is the equilibrium between liquid and solid phases in crystallization front; the diffusion rate of composite elements of InAs and GaAs in the melt supplies its homogeneity in all volume (totally mixed melt); the coefficients of component segregation of the melt change with equilibrium phase state diagram of InAs-GaAs system; thermal expansion or compression of material at phase transitions is negligible quantity; the composition of InAs-GaAs initial ingot is macro-homogeneous one.

Let's introduce the following designations: C_c , C_i , C_m are concentration parts of GaAs second component in crystal, initial polycrystalline rod and melt correspondingly; C is general concentration part of GaAs atoms in melt; C_m^0 is concentration part of GaAs in molten zone in initil time; V_c is melt volume crystallizing in time unit; V_i is volume of initial ingot InAs-GaAs, melting in time unit; V_m^0 and V_m are volumes of molten zone in initial and current time; $K = C_c/C_m$ is segregation equilibrium coefficient GaAs; L is general length of initial rods from InAs and InAs-GaAs; ℓ is length of recrystallized part of material in t moment; Z is molten zone length.

We have in limits of accepted designations:

$$C_m = \frac{C}{V_m}; \qquad \frac{dC_m}{dt} = \frac{\dot{C}V_m - \dot{V}_m C}{V_m^2};$$

$$V_m = V_m^0 - (V_c - V_i)t \; ; \qquad (1)$$

By statement of a problem Z , V_i and V_c parameters don't depend on time up to the formation of final molten zone. In this case the following ratios are carried out in region by L-Z length from seed (see fig.1A and fig.1C

$$V_m = V_m^0 \; ; \qquad V_i = V_c; \; C_m^0 = 0 \quad \text{and}$$

$$\dot{C} = V_i C_i - V_c C_m K \qquad (2)$$

Substituting (2) in (1) after set of transformations and integration we have:

$$\int_0^{C_m} \frac{dC_m}{C_i - C_m K} = \frac{V_c t}{V_m^0} = \frac{l}{Z} \qquad (3)$$

Taking under consideration the equality $K = C_c/C_m$ the equation (3) defines the component by the length of growing crystal in region from ℓ =0 up to ℓ = L-Z .

The following ratios are carried out in final region from moment of molten zone formation by Z length:

$$V_i = 0, \quad V_m = \mathrm{V_m^0} - \mathrm{V_c}t \; , \quad \dot{V}_m = -V_c \; ,$$
$$\dot{C} = -V_c \, C_m K \qquad (4)$$

We have the following after series of transformations and integrations from equation (1) taking under consideration (4):

$$\int_{C_{mf}^0}^{C_m} \frac{dC_m}{C_{mf}^0 - C_m k} = \ln \frac{V_m^0}{V_m^0 - V_c t} \qquad (5)$$

Here C_{mf}^0 is start concentration part of GaAs atoms in the melt in moment of final molten zone. Designating the length and crystallization part of the final zone melt ($V_c t / V_m^0$) in t moment by l^* and γ symbols correspondingly, let's write the equation (5) in following form:

$$\gamma \equiv \frac{l^*}{Z} = 1 - \exp\left[- \int_{C_m}^{C_{mf}^0} \frac{dC_m}{C_m K - C_m} \right] \qquad (6)$$

The definitions of l/Z and γ as C_m function (as $C_c = K \, C_m$) along whole material length treated by zone recrystallization, requires the integral solution in equations(3) and (6). The segregation coefficient of second component (k) including in both these equations depends on C_m [1]. This circumstance leads to necessity of integral calculation in (3) and (6) by numerical method with use of data of phase equilibrium state diagram of InAs-GaAs. Give gradually C_m values in required interval and define the K values conjugated with it, the integrals in (3) and (6) are solved by numerical method.

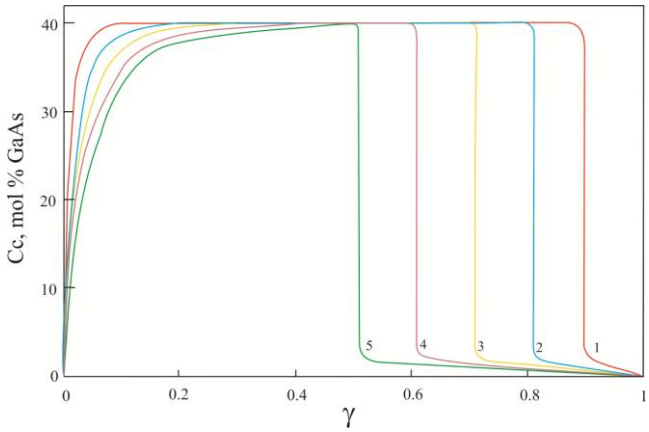

Fig.2. The calculative concentration profiles of GaAs along InAs-GaAs single crystals grown by modified zone melting method at different values of molten zone length Z. 1,2,3,4 curves correspond to values Z/L = 0,1, 0,2, 0,3, 0,4, 0,5 correspondingly. The composition for all initial ingots of solid solutions is equal to $InAs_{0.6}$-$GaAs_{0.4}$.

The character curves of GaAs concentration distribution along crystals InAs-GaAs for different Z values calculated from equations (3) and (6) taking under consideration ratios $C_c = C_m K$ are presented in fig.2. In calculations the start composition of all initial macro-homogeneous rods is equal to $InAs_{0.6}$-$GaAs_{0.4}$.

As it is seen from this figure Z operational parameter significantly influences on component redistribution at zone recrystallization of InAs-GaAs initial rod of the given composition. Moreover, the lengths of both homogeneous and heterogeneous crystal parts by composition are defined by molten zone value Z. The curve family (fig.2) directly demonstrates the potential and availability of modified method of zone melting for obtaining of solid solution single crystals InAs-GaAs with required homogeneous and alternative compositions by the way of choice of corresponding values of technological parameters (Z, C_i).

CONCLUSION

Summarizing the above mentioned one can conclude the following. The math modeling of component axial distribution in crystals InAs-GaAs grown by modified method of zone recrystallization and carried out taking under the consideration the complex character of component segregation coefficient change with melt composition gives the possibility to evaluate the optimal technological parameters (molten zone length and initial composition of feeding rod) for obtaining of solid solution crystals with given component concentration profile.

[1] *V.S. Zemskov, V.B. Lazarev.* Tverdie rastvori v poluprovodnikovix sistemax. «Nauka», Moskva, (1978) 197. (In Russian).

[2] *J. Schilz, V.N. Romanenko.* Bulk growth of Silicon-Germanium Solid Solutions, J. Materials in Electronics,V.6 (1995) 265-279.

[3] *G.Kh. Azhdarov, T. Kucukomeroglu, A. Varilci et al.* Distribution of components in Ge-Si bulk single crystals grown under continuous feeding of the melt with the second component (Si), J. Crystal Growth, 226 (2001) 437-442.

[4] *I. Kostylev, J.K. Woodacre, Y.P. Lee et al.* Melt zone growth of Ge-rich Ge1-xSix bulk single crystals, J. Crystal Growth, 377 (2013)147-157.

[5] *T.A. Campbell, M. Schweizer, P.Dold et al.* Float zone growth and characterization of Ge1-xSix (x<10 at%)single crystals, J. Crystal Growth, 226 (2001) 231-237.

[6] *N.V. Abrosimov, S.N. Rossolenko, W. Thieme et al.* Czochralski growth of Si- and Ge-rich SiGe single crystals, J. Crystal Growth, 174 (1997) 182-186.

[7] *Z.M. Zakhrabekova.* Kristalli tverdix rastКристаллы твёрдых растворов Ge-Si. Poluchenie i elektricheskie svoystva slojnoleqirovannix кристаллов Ge-Si c primesyami medi, alyuminiya I surmi, LAP LAMBERT Academic Publishing, Germaniya (2013) 139. (In Russian).

[8] *V.K. Kazimova.* Kristalli Ge-Si I ix svoystva. Poluchenie I elektricheskie svoystva tverdix rastvorov Ge-Si, slojnoleqirovannix primesyami medi, indiya I surmi, LAP LAMBERT Academic Publishing, Германия (2013) 144. (In Russian).

[9] *G.Kh. Azhdarov, R.Z. Kyazimzade.* Growth of homogeneous single crystals of Ge-Si solid solutions by the modified Bridgman method, Crystallography Reports, 50 (2005) S149-S153.

[10] *G.Kh. Azhdarov, Z.M. Zeynalov, Z.A. Agamaliyev, A.I. Kyazimova.* Growth of single crystals of semiconductor solid solutions by double feeding of the melt method, Crystallography Reports, 55 (2010)763-767.

[11] *V.M. Glazov, V.S. Zemskov.* Fiziko-ximicheskie osnovi leqirovaniya poluprovodnikov. M.: Nauka, (1967) 371. (In Russian).

Recevied: 14.09.2017

INSIGHTS INTO BIOACTIVE CONFORMATION OF MELANOTROPINS

G.A. AKVERDIEVA, N.A. AKHMEDOV, N.M. GODJAYEV
Institute for Physical Problems, Baku State University,
Z.Khalilov st.23, AZ-1148, Baku, Azerbaijan
E-mail: hagverdigulnara@gmail.com

By the molecular mechanics, molecular dynamics, quantum chemical methods and modern computer programs the structure problems of hormone-receptor interactions, deals melanotropins are considered. The conformational-electronic peculiarities, which are important for the functional activity of *α-, β-, γ-*-melanotropins and its active analog are revealed. On the basis received results the bioactive conformation of melanotropins were assessed. An α-spiral was revealed on the polypeptide chain of common for them fragment, pharmacophore -His-Phe-Arg-Trp-, provided specificity of melanotropin-receptor interaction.

Keywords: melanotropins, bioactive conformation, pharmacophore, structure-function relationships
PACS: 36.20.Ey; 36.20.Fz; 36.20.Hb

1. INTRODUCTION

α-melanotropin (H–Ser1–Tyr2–Ser3–Met4–Glu5–His6–Phe7–Arg8–Trp9–Gly10–Lys11–Pro12–Val13–H), β-melanotropin (H–Asp1–Ser2–Gly3–Pro4 –Tyr5–Lys6–Met7–Glu8– His9–Phe10–Arg11–Trp12–Gly13–Ser14–Pro15–Pro16–Lys17–Asp18-OH) and *γ*-melanotropin (H-Tyr1–Val2–Met3–Gly4–His5–Phe6–Arg7–Trp8–Asp9–Arg10–Phe11–Gly12–OH) are the cleavage products of pro-opiomelanocortic precursor (POMC), which are expressed in the pituitary gland of the cold-blooded vertebrates, bird and mammals and are found also in other cells such as neutrophils, monocytes, melanocytes, fibroblasts and keratinocytes [1,2]. The melanotropins stimulate physiological and morphological changes of skin and hair coloration [3-5]. However, the biological role of these hormones does not seem to be restricted only by a melanotropic action. A number of their other activities have been discovered, such as a lipolytic, steroidogenetic activities, sodium-uretic effects, a positive chronotropic influence on the nervous system and muscular systems. Injection of *β*-melanotropin induced a tachycardia effect and a hypersensitivity, as well as behavioural reactions. Neurotransmitting and neuromodulating activities of melanotropins were demonstrated. The effects of β-melanotropin on memory, concentration abilities were reviewed. It is shown *γ*-melanotropin decreases the effects of *β*-endorphin. It is found α-melanotropin is also a peripheral, integrative regulator of glucose and fat metabolism [6-9]. Melanotropins have also anti-inflammatory properties [10]. It is proposed -His-Phe-Arg-Trp- fragment of these peptides may be considered as the message sequence [11].

Thus above mentioned forms of melanotropins show both different and similar biological functions. The wide spectrums of diverse biological activities of melanotropins are undoubtedly connected to the conformational flexibility of these hormones that is necessary to produce structures complementary to active sites of various receptors. However, this polyfunctionality does not interfere the high sensitivity and specificity of each particular action of these hormone peptides.

The development of representations about the action mechanism of biologically active peptides, the understanding of the reasons of activity and selectivity of pharmaceutical substance binding with a biological target, is possible thanks to structure-function investigations. Many experimental works are devoted to the structure-function investigations of peptides of this family. Note that none of these methods used led to a sufficiently clear, and even more so to a reasonable quantitative representation of the structure of these molecules, but only allowed the authors to make a number of considerations about some of their probable features. In the presented work using the molecular modeling, the comparative conformational analysis of *α*-melanotropin, *β*-melanotropin and γ-melanotropin and their active analog H-His-Phe-Arg-Trp-OH, sequence of which corresponds to melanotropins pharmacophore was performed, as result the common to these molecules the optimal conformational features were found. The conformation-electronic peculiarities, which are important for the functional activity of these peptides, are revealed. On the basis received results the bioactive conformation of melanotropins was assessed.

2. METHODS

Conformational energy calculations were made on IBM computer using the version of ECEPP (Empirical Conformational Energy Program for Peptides) [12, 13]. The program was developed from the matrix method principle of Hermans and Ferro [14]. The investigations were carried out within molecular mechanics framework as described in [15, 16]. The conformational potential energy of the peptides was calculated as the sum of the independent contributions of nonvalent (E_{nv}), electrostatic (E_{el}), torsional (E_{tor}) interactions and hydrogen bonds (E_{hb}) energies. A rigid valence scheme of the molecule was assumed, namely, the searches were made only on torsional angles. The conformational state of each amino acid residue is characterized by backbone (φ, ψ, ω) and side chain (χ_1, χ_2, χ_3,...) dihedral angles. The term "conformational state" or "conformation", used in the following analysis, will always imply exact quantitative characteristics of the geometry of the residue or the fragment. The backbone was described by the "shape" symbols *e* and *f* corresponding to extended and folded configuration of virtual bonds C^{α}_{i}- C^{α}_{i+1}- C^{α}_{i+2}- C^{α}_{i+3}, respectively. The nomenclature and conventions adopted are those recommended by IUPAC-IUB [17].

The molecular dynamics of dermorphin was spent

131 H.Javid ave, AZ-1143, Baku
ANAS, G.M.Abdullayev Institute of Physics
E-mail: jophphysics@gmail.com

with use of force field AMBER in the temperature interval 293-313K with step 5K during 10 nanoseconds by means [18]. Procedure solvation with application of model of water in the set spherical volume TIP4P [19] has been used. The quantum-chemical calculations of these molecule were conducted by method CNDO [20], used the demonstration version of software package HyperChem (http:// www.hyper.com).

3. RESULTS AND DISCUSSION

The polyfunctionality of melanotropins points to the existence of a restricted number of definite spatial structures of these peptides in the conformational equilibrium. For this reason, the investigation of the structure-function relationship of these molecules at the molecular level should start from an elucidation of the complete set of low-energy states of the molecules, which may prove biological active.

We previously have considered in detail the spatial structure of investigated melanotropins [21,22,23]. In first step the conformational possibilities of active analog H-His-Phe-Arg-Trp-OH have been investigated on the basis of knowledge of low-energy states of monopeptides. It is found that low-energy conformations of this molecule have spiral form of tetrapeptide backbone or β-turn on dipeptide segment Arg-Trp. In these structures the positively charged side chain atoms of Arg and the negatively charged C-terminal carboxyl group are spatially close, that is accompanied by effective electrostatic contacts and the formation of hydrogen bonds. The nonvalent interactions of the side chains of His, Phe and Trp residues are the major contribution to the conformational energy of this molecule. These residues effectively interact both with each other and with the amino acid residue at the 3-th position.

Conformational analysis of the melanotropin molecules was carried out through a fragmental calculation, by studying of the conformational possibilities of the complicated molecular fragments. The calculations were based on the universal sets of low-energy conformation states of free amino acids. The pattern of division of a given amino acid sequence into fragments is a purely technical procedure of calculations, which was shown to have no influence on the final set of low-energy conformations.

As a result, only a very restricted set of of low-energy conformations was isolated from a great number of analysed combinations of the preferable states of the fragments, which model possible structures of investigated molecules. Conformational analysis *leads to* a unique structure of the tridecapeptide Ser1-Val13. The most probable structures of the α-melanotropin have the relative energies in a fairly wide interval 0-10.0 kcal/mol. The energy gap between the most preferred structures with a relative energy of 0.0 and 1.1 kcal / mol and subsequent conformations is approximately 8-9 kcal /mol. It is no mere chance that a steric complementarity of all parts of the molecule, are observed only for a small number of combinations of most favourable conformations of separate fragments. This fact seems to be responsible for a strictly determinative mechanism of a spontaneous and faultless folding of the amino acid sequence under native conformations and a rapid shifting of conformational equilibrium towards an actual structure of the hormone induced by a specific receptor or by other inter-molecular forces. In the optimal structures of this molecule belonging to *ffffff*-shape the fragment Met4-Gly10 has α-spiral structure, in other structures this part of molecule has *fffeee, fffeef, fffeff, fffefe*-shapes of backbone. It can be mentioned that in preferable structures of this molecule the central site, N- and C-terminal segments of molecule are close in space. The increase in energy during the transition from the optimal structures to the other is due to the loss of stabilizing contacts between the N- and C-terminal parts of the chain, i.e., the weakening of long-range interactions. In the optimal structures, the interaction of fragments Tyr2-Met4 and Pro12-Val13 is equal to 8.5kcal/mol. With respect to average interactions, all optimal conformations are approximately equivalent, so one can expect that the conformational capabilities of the molecule increase at interaction with different receptors, in which their specificity manifests itself. These structures may prove to be relevant when the sequence of this molecule will be embedded into a polypeptide chain or changing the nature of the nearest residues on either side of the Met4-Gly10 fragment. In the low-energy structures of the molecule the side chains of Glu5, Arg8 and Lys11 are oriented from the molecule to the environment and the side chain of Glu5 is closely approached to the side chain of Lys11 and is away from side chain of Glu8.

Most probable structures of the β–melanotropin have the relative energies in a sufficiently wide interval 0-12.0 kcal/mol. There are only nine such variants. Such an extremely sharp energy range of conformations of Asp1-Asp18, which is produced by joining of low-energy conformations of free fragments into a united chain, undoubtedly indicates that strong stabilizing contacts between far-ranging residues might work in unique situations, with maximum compact packing and consistency of interactions within every fragment of the natural octadecapeptide. Low-energy conformations of β -melanotropin may be divide on several groups, in which the relative structures are combined. Just so, three groups consist of conformations, which have identical shape of the peptide skeleton and stabilize, as rule, by identical interactions and have close values of dihedral angles of amino acid residues. Each group is characterized by the definite conformational state of central segment Met7-Trp12: *fffef, fffef* and *fffff,* correspondently. The third group in which the amino acids of this fragment form spiral conformation, represent special interest. For β -melanotropin the α -spiral form of the peptide skeleton of fragment Met-Glu-His-Phe-Arg-Trp is realized in the optimal conformation with $E_{rel.}$= 4.2 kcal/mol. The values of intra- and inter-residue dispersion and electrostatic interactions, as well as of torsional energy are indicative of the alternative nature of stabilization of different low-energy structures. Thus, the global conformation of this molecule exhibits an inter-residue dispersion energy which is 5.0 kcal/mol lower than that in the next low-energy structure with $E_{rel.}$= 0.5 kcal/mol. This provides for a sensitivity of the conformational equilibrium to external factors, shifting it towards the second structure by a change from a polar medium to a more hydrophobic one. Conformation, which is inferior to the global structure by

8.7 kcal/mol, appears to have few prospects at first sight. The high energy of this structure results from a comparatively small contribution of inter-residue electrostatic interactions. However, this conformation exhibits the most favourable dispersion contacts and therefore may be expected to become the most preferred one in a strongly polar medium, when electrostatic interactions do not play a significant part. Both the nonvalent and electrostatic interactions of the side chains of Phe and Trp residues are the major contribution to the conformational energy of this molecule. These residues effectively interact both with each other and with the amino acid residues at other positions of this sequence. In the preferable conformations of this molecule the positive charged amino group of the side chains of Lys6, Arg11, Lys17 and the negatively charged atoms of the side chain of residue Glu8 and COO^- terminal group interacts by effective electrostatic interactions. Such structures are stabilized also by intensive dispersion contacts of the backbone atoms and are characterized by compactness of the spatial structure, as evidenced by the value of the distance between the heavy atoms. Besides, these structures are stabilized also by the hydrogen bonds between the backbone atoms.

The most probable structures of γ-melanotropin have relative energies in the interval of 0-10 kcal/mol. There are 14 such variants. The results of calculations shows that this peptide hasn't the clean-cut fixed threedimentional structure, yet it make be realized by restricted number of definite spatial structures in the conformational equilibrium. As it turned out the fragment Tyr1-Gly4 of this peptide is flexible. The conformational-rigid nucleation is found on the fragment His5-Arg10. The form of backbone of the central fragment Arg7-Arg10 defines the basic stabilizing forces of whole molecule. The global and four relative conformations, which belong to identical shape, contain the α-spiral on the fragment His5-Arg10 (*fffff*-shape). As for α- and β - melanotropin, in such conformations of γ-melanotropin the central site and C-terminal segments are close in space. In the low-energy structure with $E_{rel.}$ = 3.6 kcal/mol and 15 relative conformations the fragments Tyr1-Gly4 and Phe 6-Phe11 have folded structure. β-turn is found on the segment His5-Phe6 of these structures. The fragment His5-Arg10 of these structures has *effff*-shape of backbone. The calculations show that in the optimal structures of this molecule the residues Phe6 and Trp8 participates in the effective interactions with charged residues Asp9 and Arg10. As can be seen from these results, the stability of spatial structure of this peptide molecule is determined by mutual position of the aromatic side chains of the residues Phe6, Trp8 and charged groups of the residues Asp9, Arg10.

Then the established low-energy conformations of all melanotropins were subjected to the molecular dynamics simulations of 10 ps. As a result of simulation process, the ranges of change of dihedral angles and distances between atoms of amino acid residues are defined. The results of molecular dynamics demonstrate the conformational rigidity of the peptide backbone of tetrapeptide fragment His-Phe-Arg-Trp and the mobility of functional groups of the side chains. The quantitative estimation of the distances between the atoms shows that at modelling the mentioned part of the molecules preserves the spiral structure throughout molecular dynamics simulation; the structure of this part of molecules upon termination of modelling process practically does not differ from the initial stage. The dispersion contacts between the atoms of backbone of the amino acid residues His and Trp are invariable, the distance between C^{α}- atoms of the specified residues does not exceed 12Å during simulation. It is possible to assume the conformational stability of specified tetrapeptide fragment plays important role in functional activity of melanotropin molecules and defines the specificity of its interaction with the receptor. It is shown in the optimal structures of investigated molecules the aromatic side chains of residues Phe and Trp have conformational mobility because of localization on surface of the peptide molecules and therefore may be in the specific orientations, which are favourable for interaction with receptor. It is found that the amplitudes of the fluctuations of the atoms of these residues in the aqueous environment are decreased. You can come to the conclusion that the atoms in the side chain of these residues contact with a certain number of water molecules that limits the mobility of these residues. It can be assumed that at interaction with receptor the side chains of these residues will be free from water molecules and may be involved in the intermolecular contacts in the role of the substrate. This assumption is confirmed by the work [24], which suggests that the aromatic groups of these residues may be involved as a donor or acceptor at the formation of hydrogen bond with the less acidic hydroxy groups of the receptor. The topography of the pharmacophore revealed the significance of the indole ring of the Trp side chain at interactions with melanocortin MC1 receptor [25]. Note that the side chain of residue Arg of central tetrapeptide showed some dynamics in simulation process, which enables, apparently, them to participate in the receptor selectivity of these molecules. This assumption is confirmed by the work of [26], which suggests that this positive charched residue may be involved in electrostatic interactions with the negative charched residues Asp or Glu (at mutation) of MC2 receptor.

The bioactive conformation of α-, β- and γ-melanotropins was assessed by a comparative conformational analysis by pairwise cross comparisons of the low energy conformations found for melanotropins and their active analog H-His-Phe-Arg-Trp-OH, corresponding to their pharmacophore. Subsets of conformations common to these peptides were pairwisely compared for similarity. Comparisons were carried out superimposing residues of pharmacophore -His-Phe-Arg-Trp- of melanotropins with their active analog, respectively. Thus, an *rmsd* (root-mean-square deviation) values of the putative bioactive conformation of melanotropins with all conformations of the subset of low-energy conformations of the active analog were computed. In the structures of α-melanotropin residues 6–9 exhibit *rmsd* of 0.75 Å, of β- melanotropin residues 9-12 exhibit *rmsd* of 0.82 Å, of γ-melanotropin residues 5-8 exhibit *rmsd* 0.79 Å when these residues are compared with mentioned active analog. It was found the spiral conformation of the molecule H-His-Phe-Arg-Trp-

OH, is realized in the optimal conformations of melanotropin molecules. Such conformations of melanotropins showed a common properties. Indeed, the selected structures among all the common to the investigated active peptides are stabilized by a hydrogen bond between the hydroxyl group of the side chain of residue His and the carbonyl oxygen of the residue Trp, the positive and negative charged side chain atoms take part in the effective electrostatic contacts. The dihedral angles of most similar structures to the putative bioactive conformation found in the set of low-energy structures of the active analog H-His-Phe-Arg-Trp-OH of melanotropins and α-, β- and γ-melanotropins are listed in Table 1 and Table 2 These structures are shown in Fig.1. The superimposition of the putative bioactive conformation of α-melanotropin, that exhibits the smaller *rmsd* with the spiral structure of the active analog H-His-Phe-Arg-Trp-OH of melanotropins, is shown in Fig.2. The superimposition of the putative bioactive conformations of *α*- and *β*-melanotropins, that exhibits the smaller *rmsd* with the spiral structure of the active analog H-His-Phe-Arg-Trp-OH of melanotropins is shown in Fig.3. The superimposition of the putative bioactive conformations of *β*- and *γ*-melanotropins, that exhibits the smaller *rmsd* with the spiral structure of the molecule H-His-Phe-Arg-Trp-OH is shown in Fig4.

Table 1.

Backbone dihedral angles (in degrees) of the putative bioactive conformation of active analog H-His-Phe-Arg-Trp-OH of melanotropins

Molecule H-His-Phe-Arg-Trp-OH			
Amino acid residues	φ	ψ	ω
His5	-62	-37	176
Phe6	-75	-35	-160
Arg7	-73	-40	-177
Trp8	-90	-45	-172

The conformational-electronic peculiarities, which are important for the functional activity of investigated peptides are revealed too. It was found that the bioactive conformations of melanotropins are characterized by specific distribution of electron density, that is reflected on the values of effective charges of atoms of the functional residues.

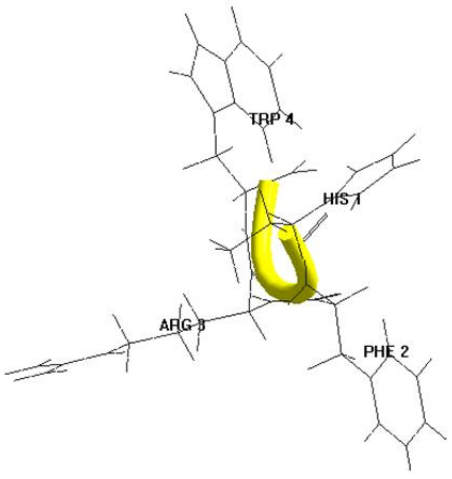

(a)

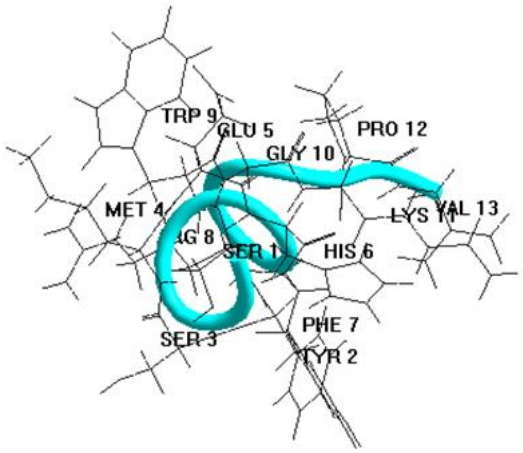

(b)

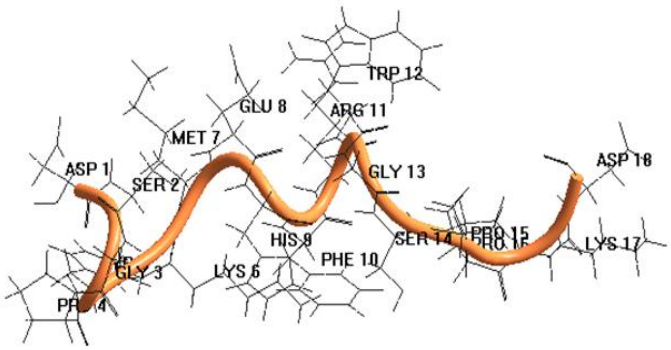

(c)

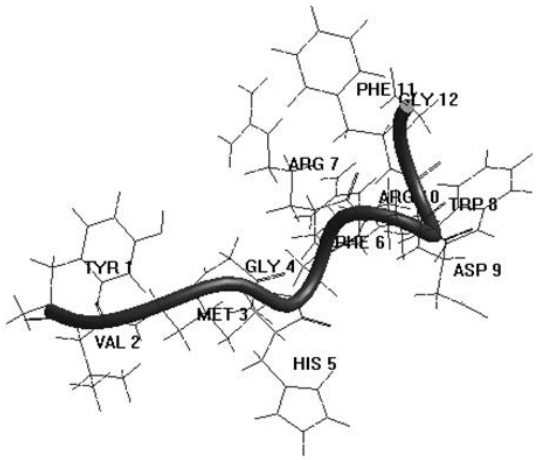

(d)

Fig.1. The putative bioactive conformation of active analog H-His-Phe-Arg-Trp-OH of melanotropins (a), *α*- melanotropin (b), *β*-melanotropin (c) and *γ*-melanotropin (d).

It was found that the distribution of charges on the atoms of pharmacophore elements (the side chains of the tyrosine, phenylalanine and tryptophan residues and charged group of arginine residue) in the bioactive conformation of the molecule H-His-Phe-Arg-Trp-OH and of the investigated molecules of melanotropins are similar.

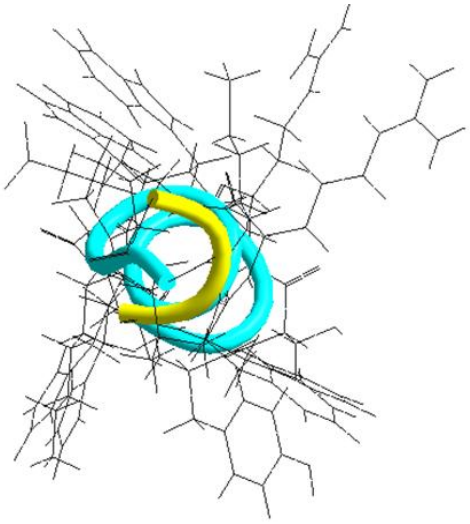

Fig.2. The superimposition of the putative bioactive conformation of α-melanotropin (in cyan), that exhibits the smaller *rmsd* with the spiral structure of active analog H-His-Phe-Arg-Trp-OH of melanotropins (in yellow).

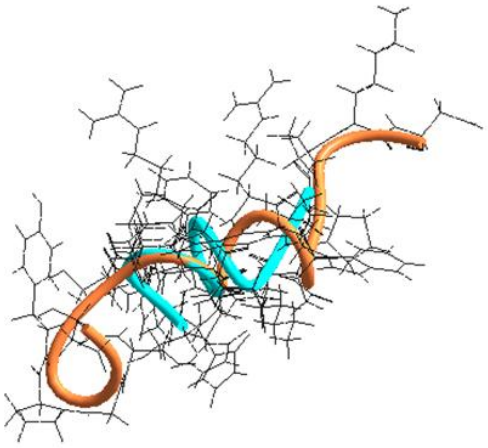

Fig.3. The superimposition of the putative bioactive conformations of α-melanotropin (in cyan) and β-melanotropin (in orange), that exhibits the smaller *rmsd* with the spiral structure of active analog H-His-Phe-Arg-Trp-OH of melanotropins.

The observed differences in the values of the charges on the certain groups of atoms as of backbone and of side chains of the residues are dictated by the specific relative position of them in each molecule. It was found that the electronic structure of the optimal conformations of these molecules is characterized by significantly lower dipole moment, than others due to the uniformity of the distribution of electron density in them. It seems that the presence of the positively charged groups of atoms in melanotropin sequences is necessary for electrostatic attraction to the negatively charged binding sites of receptors and the electrostatic repulsion from the positively charged sites of receptor. It can be assumed that the mechanism of receptor binding of melanotropins in addition to hydrophobic interactions is the formation hydrogen bonds with participation of ionizable functional groups of these molecules.

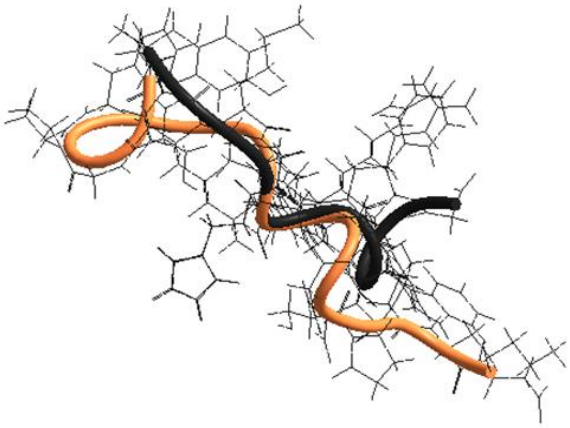

Fig.4. Superimposition of the putative bioactive conformations of β-melanotropin (in orange) and γ-melanotropin (in black), that exhibits the smaller *rmsd* with the spiral structure of active analog H-His-Phe-Arg-Trp-OH of melanotropins

The received results are in agreement to the data of the theoretical and experimental research of the melanotropins. The available experimental studies of the spatial structure of melanotropins are limited to works on CD-, NMR- and IR-spectroscopy, and fluorescence analysis [27-30]. Based on these investigations it is assumed that the N-terminal fragment of ACTH, which sequence includes α-melanotropin, has an ordered structure close to the α-helical structure, which is stabilized upon transition to non-aqueous solutions simulating the natural environment of membrane proteins. A conclusion was also made on the significant conformational rigidity of the fragment of His-Phe-Arg-Trp, which determines the melanocyte-stimulating activity of melanotropins. It was estimated from the fluorescence spectra that the distance between the aromatic rings of the residues Tyr and Trp is 9 Å. In [31], where a secondary structure for the α-, β-melanotropins was predicted by Chow and Fasman's method, the content of the α-helix on the fragment Met-Glu-His-Phe-Arg-Trp-Gly is also indicated. The possible topographic role of the residues of the fragment His-Phe-Arg-Trp, that may be explained by similar conformational effects of the side chains are discussed in [32]. These data explain the covariant character of replacements for amino acid residues Glu in 5-th and Gly in 10-nd positions of α-melanotropin, Glu in 8-th and Gly in 13-th positions of β -melanotropin, Gly in 4-th and Asp in 9-th positions of γ-melanotropin. Apparently, the maintenance of the function of these hormones is found to be possible if above indicated residues are close in space and act on the same points of receptors by functional groups. Evidently, for the same functions of melanotropins their close central segment corresponding to mutacion-stable sequence Met-Glu(Gly)-His-Phe-Arg-Trp through its structure organization are responsible. The conformational-electronic similarity of "common fragment" His-Phe-Arg-Trp and the data of its biology activity allow think this segment provides the specificity of melanotropin-receptor interaction.

Table 2.

Backbone dihedral angles (in degrees) of the putative bioactive conformation of α -, β- and γ-melanotropins

α- melanotropin				β- melanotropin				γ- melanotropin			
Amino acid residue	φ	ψ	ω	Amino acid residue	φ	ψ	ω	Amino acid residue	φ	ψ	ω
				Asp1	-71	151	-179				
				Ser2	-57	131	-178				
				Gly3	127	-85	168				
Ser1	-99	165	-177	Pro4	-60	-43	174				
Tyr2	-58	-37	-178	Tyr5	-108	143	-173	Tyr1	-107	141	176
Ser3	-76	-31	-173	Lys6	-100	119	178	Val2	-123	-71	180
Met4	-130	-73	175	Met7	-135	-53	175	Met3	-133	168	179
Glu5	-88	-42	-170	Glu8	-86	-31	-169	Gly4	-80	61	180
His6	-73	-55	176	His9	-67	-38	-177	His5	-57	-37	174
Phe7	-90	-58	170	Phe10	-78	-50	-168	Phe6	-80	-45	-151
Arg8	-95	-45	-175	Arg11	-80	-40	-176	Arg7	-65	-40	-178
Trp9	-100	-58	-174	Trp12	-99	-48	-174	Trp8	-88	-40	-170
Gly10	-70	-49	-178	Gly13	-70	-49	-179	Asp9	-77	-49	180
Lys11	-119	98	172	Ser14	-97	136	176	Arg10	-83	-67	-164
Pro12	-60	138	176	Pro15	-60	135	177	Phe11	-77	-46	-173
Val13	-137	158	-	Pro16	-60	-57	178	Gly12	90	89	-
				Lys17	-121	-67	-179				
				Asp18	-122	158	-				

4. CONCLUSION

The stability of spatial structure of melanotropins is defined by mutual position of pharmacophore elements: the aromatic rings the side chains of the tyrosine, phenylalanine and triptophan residues and charged group of Arg and is characterized by a specific distribution of electron density, which plays an important role in the interaction with the receptor. The conformational-electronic similarity of the "common fragment" His-Phe-Arg-Trp of melanotropins suggests that the helical structure of this tetrapeptide provides the specificity of melanotropin-receptor interaction. It can be assumed that the mechanism of receptor binding molecules melanotropins is to form the hydrophob interactions of aromatic rings and electrostatic contacts with participation of ionizable functional groups of these molecules.The received structural data are of interest for the study of the mechanism of the physiological effect of the melanotropins and can be used in the design of new artificial analogues.

[1] *A.J. Kastin.* Handbook of Biologically Active Peptides, Academic Press. ISBN 978-0-12-385096-6. (2013)838–844.

[2] *H.D. Jakubke, N. Sewald.* Peptides from A to Z: A Concise Encyclopedia. John Wiley & Sons. ISBN 978-3-527-62117-0(2008)216.

[3] *K. Rousseau et al.* Proopiomelanocortin (POMC), the ACTH melanocortin precursor, is secreted by human epidermal keratinocytes and melanocytes and stimulates melanogenesis. FASEB. J. 21(2007)1844–1856.

[4] *R.P. Hill, S. MacNeil, J.W. Haycock*. 2006. Melanocyte stimulating hormone peptides inhibit TNF-alpha signaling in human dermal fibroblast cells. Peptides 27:421–430.

[5] *R.P. Hill, P. Wheeler, S. MacNeil, J.W. Haycock.* Alpha-melanocyte stimulating hormone cytoprotective biology in human dermal fibroblast cells. Peptides 26(2005)1150–1158.

[6] *K. Eerola, W. Nordlund, S. Virtanen, A.M. Dickens et al.* Lentivirus mediated α-melanocyte stimulating hormone overexpression in the hypothalamus stimulating hormone overexpression in the hypothalamus decreases diet induced obesity in mice. J. Neuroendocrinol, 25(2013)1298–1307.

[7] *M.B. Brennan, J.L. Costa, S. Forbes, P. Reed et al.* Alpha-melanocyte-stimulating hormone is a peripheral, integrative regulator of glucose and fat metabolism. Ann N Y Acad Sci., 994(2003)282-87.

[8] *J.E. Royalty, G. Konradsen, O. Eskerod, B.S. Wulff, B.S. Hansen.* Investigation of safety, tolerability, pharmacokinetics and pharmacodynamics of single and multiple doses of a long-acting α-MSH analogue in healthy overweight and obese subjects. J Clin Pharmacol, 54(2014)394-404.

[9] *A. Vehapoğlu, S. Türkmen, Ş. Terzioğlu.* Alpha-Melanocyte-Stimulating Hormone and Agouti-Related Protein: Do They Play a Role in Appetite Regulation in Childhood Obesity? J.Clin Res Pediatr Endocrinol. 8(2016) 40–47.

[10] *J.M. Lipton, A. Catania.* Anti-inflammatory influence of the neuro immunomodulator alpha-MSH. Immunol. Today 18(1997)140–145.

[11] *M. Cai, V.J. Hruby.* Design of cyclized selective melanotropins, *Biopolymers,* 2016, 106(6) 876-883

[12] *N.M. Godjayev, I.S. Maksumov, L.I. Ismailova.* Program of semiempirical calculations of conformations of molecular complexes, J.Struct.Chem., 4(1983) 147-148 (in Russian)

[13] *G.A. Akverdieva.* Improvement of program of

calculation of molecular conformation. Theoretical and applied aspects of modern science. Collection of scientific papers of VI International Scientific-Practical conference, Belgorod (2015) 11-14 (in Russian).

[14] *J. Hermans and D. Ferro.* Representation of a protein molecule as a tree and application to modular computer programs which calculate and modify atomic coordinates, Biopolymers, 10(1971)1121-1129.

[15] *N.M. Godjayev, S. Akyuz, G.A. Akverdieva.* A molecular mechanics conformational study of peptide T, J. Mol. Structure, 403 (1997) 95-110.

[16] *G.A. Akverdieva, N.M. Godjayev, S. Akyuz.* Conformational dynamics of peptide T molecule. Journal of Molecular Structure, 609 (2002) 115-128.

[17] IUPAC-IUB. Quantities, Units and Symbols in Physical Chemistry, Blackwell Scientific, Oxford (1993) 168.

[18] *K.V. Shaitan, S.S. Saraykin.* Molecular dynamics method, 1999. http:// www.moldyn.ru (in Russian).

[19] [19] *H.W. Horn, W.C. Swope, J.W. Pitera et al.* Development of an improved four-site water model for biomolecular simulations: TIP4P-Ew. J. Chem. Phys. 120 (2004) 9665-9678.

[20] *N.L. Allinger, Y. Yuh.* QCPE 395, Quantum chemistry program exchange, Indiana Univ., Indiana, 1982

[21] *N.A. Akhmedov, E.M. Popov.* Structure organization of theα-melanotropin molecule. Molecular biology, 23 (1989) 249-254 (in Russian).

[22] *N.A. Akhmedov, G.A. Akverdiyeva, N.M. Godjayev, E.M. Popov.* Theoretical conformational analysis of brain peptides. Int.J.Peptide and Protein Res., 27 (1986) 95-112.

[23] *G.A. Akverdiyeva.* Conformational aspects of the action of β- and ϒ- melanotropins. Istanbul Üniv. Fen Fak. Astronomi ve Fizik Der., 61(1996) 61-66.

[24] *V.J. Hruby.* Truncation studies of α-melanotropin peptides identify tripeptide analogues exhibiting prolonged agonist bioactivity, Peptides, 17(1996)995-1002.

[25] *C. Haskell-Luevano, L.W. Boteju, H. Miwa, C. Dickinson.* Topographical modification of melanotropin peptide analogues with β-methyltrytophan isomers at position 9 leads to differential potencies and prolonged biological activities, Journal of Medicinal Chemistry, 38 (1993) 4720-4729.

[26] *M. Asai, S. Ramachandrappa, M. Joachim, Y. Shen et al.* Loss of function of the melanocortin 2 receptor accessory protein 2 is associated with mammalian obesity. *Science,* 341 (2013) 275–278

[27] *M. Löw, L.D. Kisfaludy, Gy. Hajos, L. Sprorny et.al.* Conformation activity relationships of corticotrophin segments. Acta biochem.et biophys. Acad.Cci.hung, 16 (1981) 105-108.

[28] *D. Greff, F. Toma, S. Fermandijan, M. Löw, L. Kisfaludy.* Conformational studies of corticotropin 1-32 and constitutive peptides by circular dichroism. Biochimica et Biophysica Acta, 439 (1976) 219-231

[29] *F. Toma, S. Fermandijan, M. Löw, L. Kisfaludy.* ^{13}C-NMR studies of ACTH: Assignment of Resonances and conformational features. Biopolymers, 20 (1981) 901-913.

[30] *F. Toma, V. Dive, H. Lam-Thanh F. Piriou et al* . Conformational analysis of corticotropin (ACTH) and and conformation-activity relationship. Biochimie, 1981, vol.63, p. 907-910.

[31] *M.D. Jibson, C.H. Li.* Secondary structure prediction of anterior pituitary hormones. Int.J.Peptide Protein Res., 14 (1979)113-122.

[32] *M. Minying Cai, U.K. Marelli, J. Bao, J.G. Beck.* Systematic Backbone Conformational Constraints on a Cyclic Melanotropin Ligand Leads to Highly Selective Ligands for Multiple Melanocortin Receptors. J. Med.Chem., 58 (2015) 6359-6367.

Recevied: 28.09.2017

DIELECTRIC DISPERSION OF GLYCINE WATER SOLUTION ABSORPTION

S.T. AZIZOV [1], O.A. ALIYEV [2]
[1]Institute of Physics of Azerbaijan National Academy of Sciences, H.Javid ave.,33, AZ 1143, Baku, Azerbaijan
[2]Institute of Physics of Azerbaijan National Academy of Sciences, H.Javid ave.,33, AZ 1143, Baku, Azerbaijan
e – mail: [1]samir_azizov@mail.ru

The dielectric coefficients of one-molar water solution of water and glycine at temperature from 20°C up to50°C in five frequencies in centimetric range are measured. The dielectric spectra taking under consideration other frequencies given in reference are studied.

It is shown that Kirkwood model in which the continuous structures of water-soluble amino-acids are accepted in the capacity of medium consisting of water and bipolar molecules (zwitter-ion) of monomer acid should be revised again.

Keywords: dielectric spectroscopy, molecular spectroscopy, glycine water solution dielectric properties
PACS: 30.00.00; 33.20. – t; 33.20.Bx

INTRODUCTION

The dielectric properties of glycine water solutions are investigated many times [1-14]. The accepted description of equilibrium and dynamic characteristics is based on empiric ratios:

$$\varepsilon_{os} = \varepsilon_{ow} + \delta C \equiv \varepsilon_{ow} + \left[(\varepsilon_{os} - \varepsilon_{ow})C^{-1}\right]C, \quad (1)$$

$$\varepsilon_s^{'} - j\varepsilon_s^{''} = \varepsilon_{os} + \delta C(1 + j_{\omega\tau_1})^{-1} + (\varepsilon_o - \varepsilon_{ow})(1 + j_{\omega\tau_2})^{-1} \quad (2)$$

where C and τ_1 are molar concentration and time, “s” and ”w” indexes are related to solution and water, $\tau_1 > \tau_2$ the rest designations have the usual meaning.

Expression (1) is reliably approved by experiments. The distance r = 3,2 $Å$ between dipole charges in well coincidence with r = 3.3 $Å$ which is the distance between zwitter charges of glycine ion found for $^{+}NH_2CH_2COO^{-}$ crystal by X-ray method [15]. This result is considered as the confirmation [10] introduced by Kirkwood [5] on the base of solution model (1) in the form of single zwitter-ions homogeneously distributed in medium with undisturbed water structure.

The aim of investigations described in present article, is in establishment of quality of conformance of equation (2) to dielectric spectrum of glycine one-molar water solution on the base of eigen and reference data overlapping the wavelength range λ = 66,7 – 0,85 cm. The water is chosen in the capacity of control object.

RESULTS AND THEIR DISCUSSION

Experimental test of ratio (2) presenting the dynamic analogue (1) is mainly carried out in long-wave edge of relaxation spectrum with prior equalization of τ_2 to $\tau_в$ and some variations of short-wave region amplitude. The interval of τ_1 obtained designations exceeds the evaluation probable error. Such spread can be considered either as the sequence of initial material limitedness making difficult the spectrum unique decoding or as indication on model principal inadequacy [5].

The dielectric constants ε' and absorption indexes ε'' of water and solution are measured at λ = 5,83; 4,02; 3,23; 2,10; 1,40 cm and temperatures from 20°C up to50°C . The measured water ε' and ε" well coincide with ones calculated by equation (table 1):

$$\varepsilon^{'\prime} - j\varepsilon^{''\prime} = \varepsilon_\infty + \sum_i^3 \left(\varepsilon_{o_i} - \varepsilon_{\infty_i}\right)(1 + j\omega\tau_i)^{-1} \quad (3)$$

where ε_{o1} = 80,4; $\varepsilon_{o2} = \varepsilon_{\infty 1}$= 76,4; $\varepsilon_{o3} = \varepsilon_{\infty 2}$ = 4,58; $\varepsilon_{\infty 3} = \varepsilon_\infty$ =1,78; τ_1= 28,6: τ_2= 8,92; τ_3 = 0,046 c (20°C) [16].

Table 1

The measured ε* and calculated ε^*_{cal} by (3) the dielectric coefficients of water bidistillate at different wave lengths λ (cm) and 20°C

λ	ε'	$\varepsilon^{'}_{cal}$	ε"	$\varepsilon^{"}_{cal}$
5,83	74,0	72,9	21,2	20,9
4.02	67,8	67,4	26,9	27,3
3,23	61,6	62,2	29,8	31,2
2,10	49,7	48,9	35,6	36,4
1,40	33,2	32,5	36,4	36,3

The dispersion - absorption diagrams of studied solution constructed by our and reference data are given in the figure. In spite of big amount of publications by this system, the initial material either is absent or is given in such form that excludes the possibility of its quantitative consideration. We use ε' and ε'' tabulated in [8, 9] and presented graphically in [11].

The general number of points allows us to carry out the enough confident comparison of observable and predictable spectra by model 5in terms of S sum of standard deviations measured of ε' and ε"on calculated ones.

The analysis validation criterion is the condition $S \leq S_m$ [17] at which the deviation between test and calculation are caused by only measurement errors.

131 H.Javid ave, AZ-1143, Baku
ANAS, G.M.Abdullayev Institute of Physics
E-mail: jophphysics@gmail.com

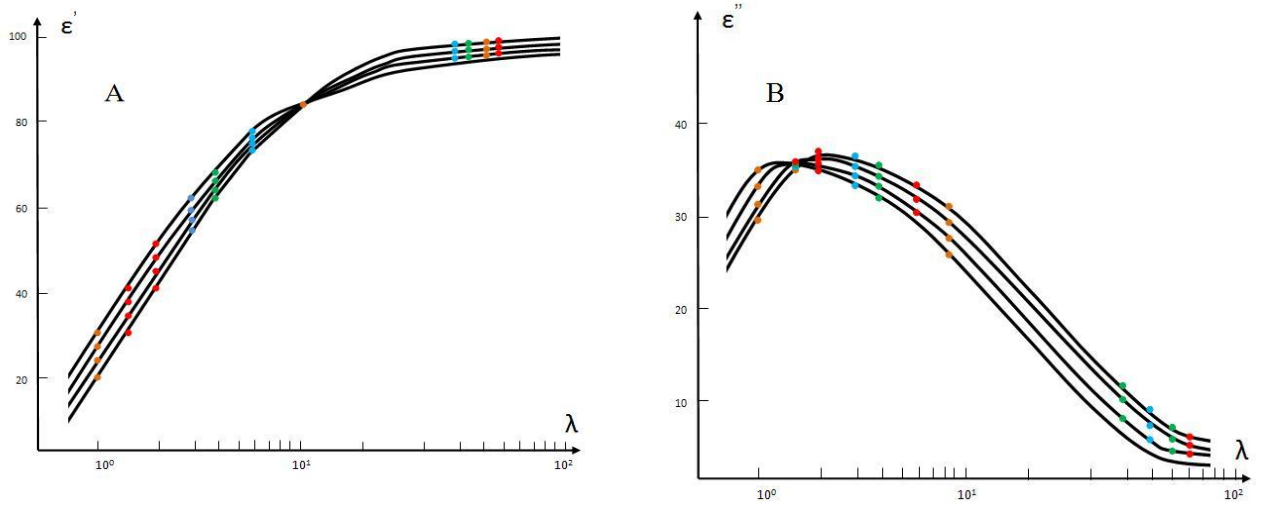

Fig. The dielectric constants ε' (A and absorption indexes ε'' (B)[1] 1M of glycine water solution in dependence on wave length λ (cm) at 20 (a); 30 (b); 40 (c); 50° (d): l (red) is our data; 2 (green) is [8]; 3(blue) is [9]; 4(brown) is [10].

Table 2

The comparison of observable and calculative spectra of one-molar glycine water solution at 20°C.

Ref.	ε_{os}	ε_{ow}	$\varepsilon_{\infty w}$	$\tau_1 \cdot 10^{12}$sec	$\tau_2 \cdot 10^{12}$sec	$S(S_m=24{,}0)$	$S_{dm}(\lambda \gg 33\text{cm})$	$S_{cm}(\lambda < 8{,}3$ cm)
[9]	102,6	80,3	5,0	72,0	9,2	114,2	4,4	109,9
[10]	102,6	76,8	5,0	72,0	9,2	60,5	9,4	68,7
[11]	102,6	68,2	3,8	43,6	8,8	48,2	22,7	25,5
[8]	103,6	27,5	_	20,0	_	894,4	281,9	612,5

All assignments suggested up to now are dissatisfied (table 2) in terms of this criterion. The distinctive agreement with experiment only in that range where authors have measured ε' and ε'' is notable and the appearance of rapidly growing divergences because of overrunning λ takes place. The parameters calculated in [9] by measurements only at four points from λ = 66,7 up to 33 cm are given in decimetric range S_{dm} = 4,4 (S_m = 8,0) and S_{cm} = 109,9 (S_m = 16,0) is given in centimetric one. According to [10] $\varepsilon_{\infty 1}$ value should be less than ε_{ow} because the amino-acid molecules behave themselves as non-polar ones at corresponding λ can be written by empiric formula:

$$\varepsilon_{\infty 1} = \varepsilon_{ow} - (\varepsilon_{ow} - 1)V \cdot C \cdot 10^{-3}, \qquad (4)$$

where V is glycine molar partial volume. In this case S increase is devalued by more than double increase of S_{dm}. The parameter set based on centimetric points leads to further decrease general S, moreover, the main contribution in S_{cm} is defined by the point at λ = 0,85 cm where S=16,3. At the same time S_{dm} increase shows the choice baselessness of τ_1= 43,6 psec instead of τ_1= 72,0 psec [9] giving the well S_{dm}. Finally, S=0,05 corresponds to experiment parameters [8] at single λ = 3,20 cm with general S=894,4 (1).

CONCLUSION

The given results allow us to confirm that the dynamic dielectric behavior of glycine one-molar water solution can't be described by ratio (2) at condition of overlapping of enough wide range wave lengths. This conclusion prejudices the use validity of ratio (1) for finding of dipole moment of monomer zwitter-ion of glycine and shows on the necessity of model revision [5] postulating the presence only two dielectrically active types of kinetic units in amino-acid water solutions.

[1] P.*B.Undre, S.N.Helambe, S.B.Jagdale, P.W.Khirade, S.C.Mehrotra.* Pramana-J. Phys., 68, 851, 2007.

[2] *B.G. Lone, P. Undre, S.S. Patil, P.W. Khirade, S.C. Mehrotra.* J. Mol. Liq., 141, 47, 2008.

[3] *A. Chaudhari, A.G. Shankarwar, B.R. Arbad, S.C. Mehrotra.* Journal of Solution Chemistry, vol.33, № 3, 2004, p. 313 – 322.

[4] *Ch.O. Gadjar, S.T. Azizov, Sh.K. Agamuradova.* Fizika, т. XIV, №2, s. 56 – 59, 2008. (In Russian).

[5] *J.G. Kirkwood.* In: "Proteins, Amino Acids and Peptides", ed. E. J. Cohn, J.T. Edsall, Reinhold. N. Y., 1943, 294.

[6] *W.L. Gent.* Trans. Farad. Soc., 50, 1954, 1229.

[7] *K. Dharmalingam, K. Ramachandran, Sivagurunathan, B.P. Undre, P.W. Khirade, S.C. Mehrotra.* Mol. Phys., 104, 2835 (2006).

[8] *O. Sandus, B.B. Lubitz.* J. Phys. Chem., 65, 1961, 881.

[9] *M.W. Aaron, E.H. Grant.* Trans. Farad. Soc., 59, 1963, 85.

[10] *E.H. Grant.* In: "Elektronenspinresonanz und andere Spektroskopischen Methoden in Biologie", Akad.-Verlag. Berlin, 1973, s. 273.

[11] *A.M. Bottreau, G. Delbos, C. Marzat, J.M. Sa1efran,*

J. Moreau. M. C. R. Acad. Sci., B276, 1973, 373.
[12] *S.T. Azizov.* Fizika, т. XVII, №2, selection: En, s. 88-90., 2011. (In Russian).
[13] *A.H. Clark, P.A. Quickenden, A.J. Suggett.* Chem. Soc. Farad. Trans., pt. 2. 70, 1974, 1847.
[14] *J.L. Salefran, D. Delbos, C. Marzat, A.M. Bottreau.* Annal Sci. Univ. Clermont, Phys., 1977, p. 199.
[15] *V.P. Pawar, S.C. Mehrotra.* J. Mol. Liq., 95, 63, 2002.
[16] *A.M. Bottreau, J.M. Moreau, J.M. Laurent, C.J. Marzat.* Chem. Phys., 62, 1975, 300.
[17] *P. Sivagurunathan, K. Dharmalingam, K. Ramachandran, B.P. Undre, P.W. Khirade, S.C. Mehrotra, Philos.* Mag. Lett., 86, 291, 2006.

Received: 08.09.2017

CELLULAR STRUCTURE IN Bi_2Te_3 THIN FOILS

K.Sh. KAGRAMANOV, E.R. ALIYEVA, I.T. MAMEDOVA, S.Sh. KAGRAMANOV, N.M. ABDULLAYEV

Institute of Physics of Azerbaijan NAS
AZ-1143 Baku, Azerbaijan
kamil.qahramanov@yahoo.com

The structures with relief having the stepped and plateau character are revealed in p-Bi_2Te_3 thin foil. The crystal deformations appearing in growth process are accompanied by the formation of deformation relief in the form of plateau surfaces and local parallel dislocations on their surfaces. The absence of changes in X-ray diffraction (XD reflexes in bulk single crystals and $A^{V}{}_2B^{VI}{}_3$ thin foils shows the deformation localization process in elastic range.

Keywords: relief, plateau, step, surface, deformation, cell, dislocation.
PACS: 62.20 Fe, 61.72.Cc, 61.72.Lk

INTRODUCTION

Last years the semiconductor crystals of Bi_2Te_3 type are the object of intensive experimental and theoretical investigations because of their unique physical properties.

The stepped structures appear in growth process and in doped layer crystals of Bi_2Te_3 type. The deformations which are character for dislocations [1-3] appear near the step in crystal volume.

The obtained theoretic results present themselves the special interest at consideration of periodically rough surfaces of multilayer structures.

Using the models of formation of cellular dislocation and fragmented dislocation structures, one can reveal the surface deformation reliefs in $A^{V}{}_2B^{VI}{}_3$ [4-6] thin foil corresponded to them on the base of following parameters:

- change character of X-ray diffraction (XD) reflexes;
- relief character with stepped and plateau types;
- correspondence of experimentally obtained structural fragments with modeling results connected with cellular structures.

The comparison of XD of crystal structures with their $A^{V}{}_2B^{VI}{}_3$ thin foils and also with theoretically calculated forms of cellular dislocation structures is the aim of our work.

EXPERIMENT

The results of modeling carried out in [4] are compared with data by the investigation of surface deformation reliefs with the help of microscope of high sensitivity: *Solver NEXT u AFM-BRUKER Nano N8 Neos*. XD investigations are carried out on diffractometer of "Bruker" D2 Phaser firm.

The thin foils for atomic force microscope (*AFM*) are prepared by the way of gradual splitting of the samples with the help of scotch. This method doesn't introduce the additional defects that are confirmed by repeat XD on which the perfect form of reflections is sometimes observed (see XD in fig.1).

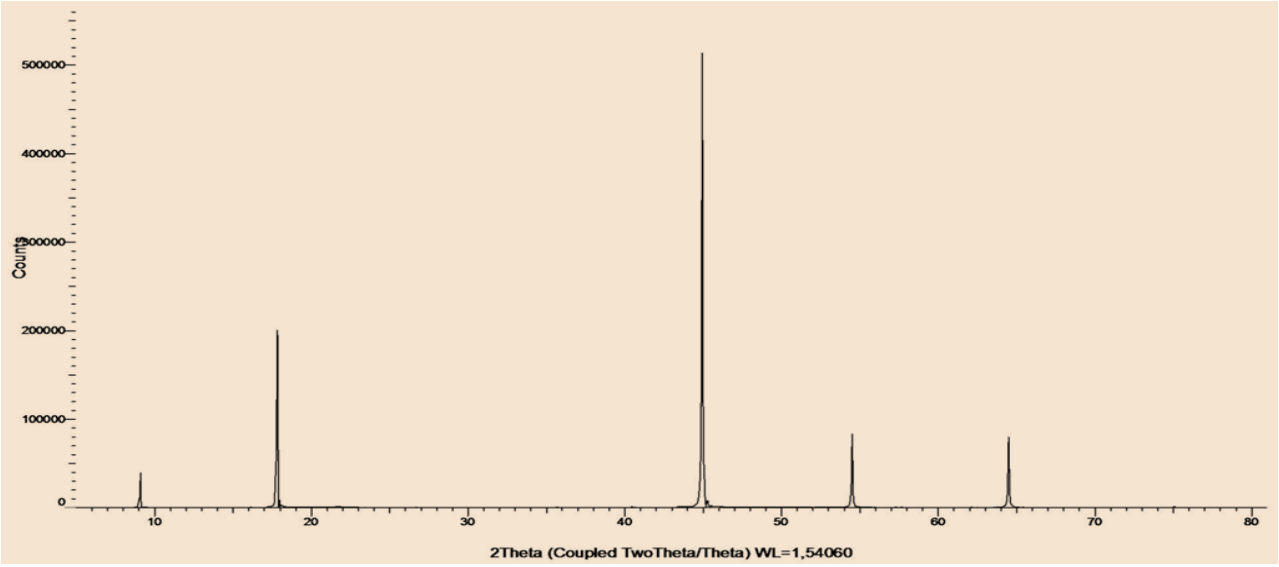

Fig.1. X-ray diffraction shot for Bi_2Te_3 thin foil. The reflexes obtained by us in bulk crystals coincide with the ones obtained in thin foil.

131 H.Javid ave, AZ-1143, Baku
ANAS, G.M.Abdullayev Institute of Physics
E-mail: jophphysics@gmail.com

The properties of such foil are studied by us first time. XD on thin foils (fig.1) are studied. The comparative analysis shows that reflexes in all samples are similar that shows the perfectness of reflection forms. The structure of all samples is perfect.

Such method is successfully applied for obtaining XD for compounds of TiX_2 (X= S, Se, Te) dichalcogenides [7].

The micro-diffractions obtained with foil plane of the investigated compounds correspond to basis plane (0001).

EXPERIMENTAL DISLOCATION STRUCTURES

The scheme of different steps and bends in planes of sliding is given in fig.2.

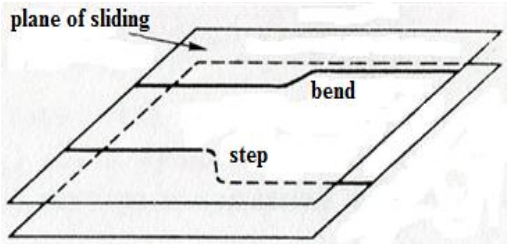

Fig. 2. Steps and bends on dislocations [8]. The cases when dislocation is in two neighbor plains of sliding, bends (blades) and another type which is step, are possible.

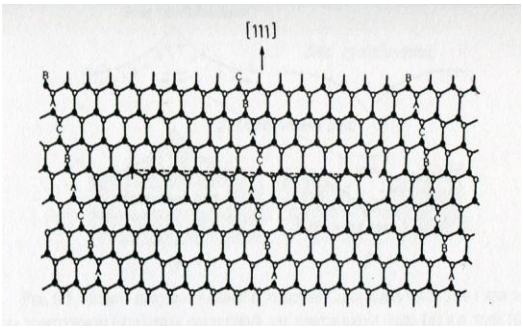

Fig.3. The cell is the type in direction of dislocation wire on atomic structure of 60% split dislocation in lattices by diamond type: the atoms of the similar elements in single crystals of *IV* group are marked by black and white circles. The detail explanation is in [8].

The positions of the steps in *(0001)* Bi_2Te_3 basal plane showing the degree of decrease from 600 up to 100 nm in Bi_2Te_3 cellular structure are given in fig.4. The relief has the stepped and plateau character.

The surface nano-objects (the places of dislocation outputs) are given in fig.5. They correspond to theoretically calculated reliefs (by G.A.Maligin data in [4-9]).

The geometric figures formed on the surfaces of semiconductor structures with nano-objects obtained by us in $A^V{}_2B^{VI}{}_3$ connect the schemes given in fig3 and fig. 4 that shows the complexity of local deformation processes presented in fig.5 and fig. 6.

The investigation results are compared with reference data on investigation of deformed relief surfaces with the help of high-resolution microscopes. The obtained thin foils are treated by deformation in preparing process. This is accompanied by the formation of deformation relief on their surface reflecting the deformation process in crystal on meso-, micro- and nano-scale levels.

The crystal deformations appearing in growth process are accompanied by the formation of deformation relief in the form of cellular structures and local parallel dislocation formations on their surface.

The deformation localization is the result of heterogeneous dislocation distribution in crystal; the surface deformation relief reflects the character of this distribution [12]. The dislocation distribution has the enough complex form at big degrees of deformation in conditions of multiple sliding. The example is the cellular dislocation structures in metals.

CONCLUSION

The investigated cellular dislocation structures in $A^V{}_2B^{VI}{}_3$ reflect the deformation localization process on different scale levels. This deformation localization can be the result of heterogeneous dislocation distribution moreover the deformation relief reflects the character of dislocation distribution in Bi_2Te_3. The absence of changes in XD reflexes in bulk single crystals and $A^V{}_2B^{VI}{}_3$ thin foils confirms the deformation localization processes in elastic range as there are XD reflexes at 2θ: 8°, 18°, 44°, 54° and 64°.

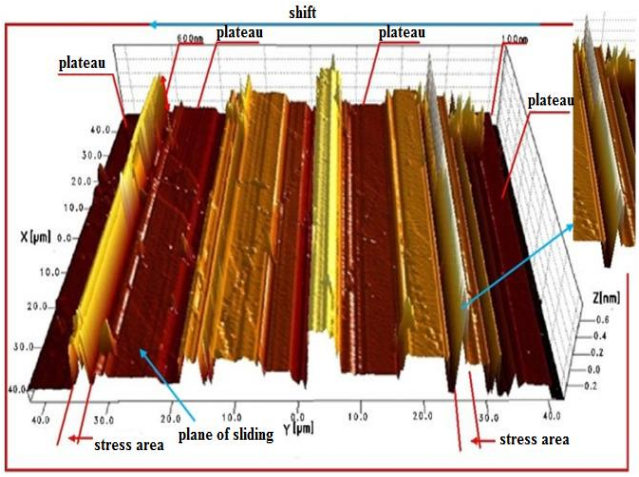

a)

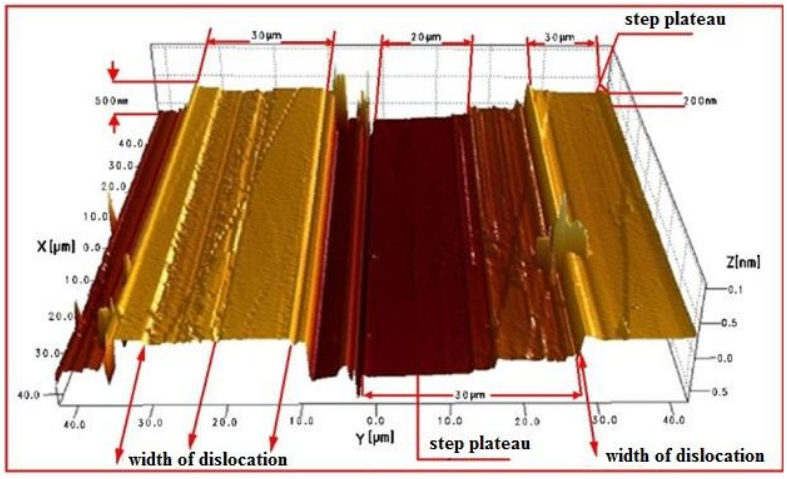

b)

Fig.4. The plateau on corrugated nano-objects in Bi_2Te_3 samples in *3D*-scale, the stress ranges and width of dislocations and plateaus are given. a) are stress ranges, plane of sliding, the height of stress range≈ 200- 300 *nm*, the width of stress range is maximal one and it is equal to ≈ 100 *nm*; b) is width of dislocation and step plateau is ≈ 30 *μm*.

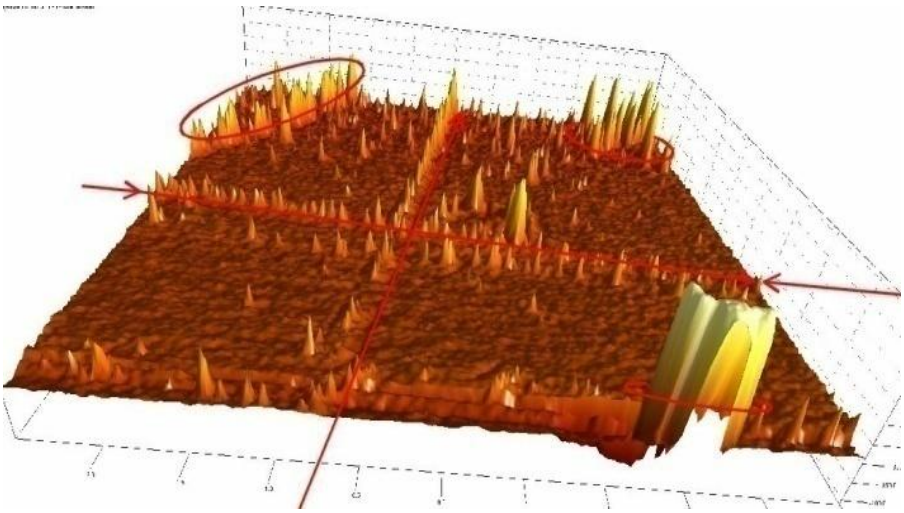

Fig.5. The dislocation structure obtained by us in Bi_2Te_3 on *(0001)* surface (the nano-objects in the form of localized nano-islands are given on top left and right in upper part of the figure) (macroscope is *AFM - BRUKERNANO)*

---

[1] *C.Y. Barlow, B. Bay, N. Hansen.* Phil. Mag. A 51, 253, (1985).
[2] Fizicheskaya Enchiklopediya-2.1990 q. Forma rosta kristalla. s.500. (In Russian).
[3] *N. Hansen, D.A. Hughes.* Phys. Status Solidi, B 149, 155 (1995).
[4] *G.A. Maliqin.* FTT, 2007, t.49, v.8, s.1392-1397. (In Russian).
[5] *G.A. Maliqin.* FTT, 2001, t. 43, 882. (In Russian).
[6] *Q. Liu, X. Huang, D.J. Lloyd, N. Hansen.* Acta Mater. 50, 3789 (2002).
[7] *E.G. Galieva, O.V. Antonova, P.E. Panfilov, A.N. Titov.* FTT, 2011, t.53, v.5, s. 984-992. (In Russian).
[8] *T. Sudzuki, X. Esinqa, S. Takeuti.* Dinamika dislokachiy I plastichnost. Moskva: «Mir», 1989, str.145. (In Russian).
[9] *G.A. Maliqin.* UFN, 169, 979 (1999). (In Russian).
[10] *G.A. Maliqin.* FTT, 48, 651 (2006). (In Russian).
[11] *G.A. Maliqin.* FTT, 43, 251 (2001). (In Russian).
[12] *Y. Kawasaki, T. Takeuchi.* Scripta Metal.14, 183, 1980.

Recevied: 12.10.2017

THERMODYNAMIC PROPERTIES OF GdTe COMPOUND

S.Z. IMAMALIYEVA[1], T.M. GASANLI[2], M.A. MAKHMUDOVA[3], F.M. SADIGOV[2]
[1]Institute of Catalysis and Inorganic Chemistry of Azerbaijan NAS
Az-1143, H.Javid ave.,113, Baku, Azerbaijan
[2]Baku State University, Az-1148, Z.Khalilov str., 23, Baku, Azerbaijan
[3]Institute of Physics of Azerbaijan NAS
Az-1143,H.Javid ave.,131, Baku, Azerbaijan

The results of thermodynamic investigation of GdTe investigation by the method of electromotive force (EMF) are presented in the work. The relative partial molar functions of gadolinium in GdTe+Gd_2Te_3 two-phase region are calculated from data obtained by method of rapid fixing of EMF. Gibb's standard free formation energy and formation enthalpy and also the standard entropy of GdTe compound are calculated on the base of obtained data and integral thermodynamic functions of GdTe.

Keywords: gadolinium telluride, GdTe, Gd_2Te_3, EMF method, thermodynamic functions.
PACS: 71.20.Be, 75.10.Nr, 75.20.-g

The rare-earth element chalcogenides are related to the number of perspective materials of electron technique. Many of them have the unique magnetic, optic and thermoelectric properties along with high thermostability and stability to strong changes of external conditions [1-4].

The development and optimization of new material obtaining processes are based on data on phase equilibriums in corresponding systems and thermodynamic characteristics of intermediate phases.

Gd-Te system [1,5] is characterized by telluride formations with GdTe, Gd_2Te_3, Gd_4Te_7, $GdTe_2$, Gd_2Te_5 and $GdTe_3$ compositions. GdTe compound congruently melts at 2098K and the rest form by peritectic reactions. The first two compounds have the cubic structure, the rest crystallize in more low-symmetry structures.

The thermodynamic properties of gadolinium tellurides aren't practically studied. Any thermodynamic data for these compounds are absent in modern reference books [6,7]. The data by standard entropy of Gd_2Te_3 are given in only electron version of "Thermal constants of substances" reference book. The standard enthalpy of this compound formation is obtained in work [8] by the method of direct synthesis from components in calorimetric bomb.

The given work is dedicated to thermodynamic properties of gadolinium monotelluride by EMF method.

EXPERIMENT AND THEIR RESULTS

The concentration chains of type

$$(-)\ \text{Gd (solid)}\ |\text{glycerine} + \text{KCl} + \text{GdCl}_3\ |\ (\text{Gd-Te})\ (\text{solid})\ (+) \qquad (1)$$

are constructed by us for study of thermodynamic properties of GdTe compound.

The melts of Gd-Te with compositions 51 and 55 at Te% (two-phase region GdTe+ Gd_2Te_3) which are synthesized by ceramic method from elementary powdery gadolinium and tellurium of high degree purity are used as right electrodes in chains of (1) type.

The synthesis is carried out in evacuated (10^{-2}Pa) quartz ampoules at 1000K. Later the melts are grinded in powder, carefully mixed and pressed in tabs which are annealed at the same temperature during ~800h. The melt phase compositions are controlled by RFA method.

The left electrolyte is prepared by the fixing of [bvbxtcrb xbcnsqmetallic gadolinium on molybdenum shunt and the right electrodes are prepared by pressing-in by Gd-Te synthesized melts grinded in powder on shunts in the form of cylinder tabs of mass ~0,5gr.

KCl glycerin solution with addition of $GdCl_3$ serves as electrolyte. Taking into consideration the inadmissibility of the presence of humidity and oxygen in electrolyte the glycerin (by ЧДА mark) are thoroughly dehydrated and degassed by pumping at temperature ~450K and the anhydrous, chemically pure KCl an $GdCl_3$ are used.

However, EMF measurements show the non-equilibrium of chains by (1) type. EMF values strongly decrease in measurement beginning during several hours in comparison with high initial ones (by order ~1000MV) up to 200÷300 values. Though later these values are reproducible ones, they aren't accepted as equilibrium ones because according to previous thermodynamic calculations they are less than predictable values in 2÷3 times.

That's why we use the simplified variant of EMF instantaneous fixing [9], i.e. the rapid fixing of EMF values which is earlier applied by us at thermodynamic investigation of ytterbium and neodymium telluride [10,11]. The heart of this method is in the fact that left electrode is in another vessel with the same electrolyte at the same temperature that the right electrodes are up to the moment of EMF measurements. EMF measurement is carried out in the moment of left electrode introduction into electrochemical system with right electrode and the maximum value of EMF is fixed. The measurements are carried out with the help of high-ohmic numerical voltmeter B7-34A in 300÷430K interval.

The measurement results are given in figure and in table. As it is seen EMF temperature dependence is linear one. The obtained experimental data are treated with the help of computer program "Microsoft Office Excel 2003" by the method of least squares. The calculations are given

131 H.Javid ave, AZ-1143, Baku
ANAS, G.M.Abdullayev Institute of Physics
E-mail: jophphysics@gmail.com

in table. The linear equation presented in the form recommended in [12] is obtained:

$$E = a + bT \pm t\left[\frac{S_E^2}{n} + \frac{S_E^2(T-\overline{T})^2}{\sum(T_i-\overline{T})^2}\right]^{\frac{1}{2}}$$

n is number of pares of E and T values correspondingly; S_E and S_b are dispersions of separate measurements of EMF and b coefficient; $\overline{T}$ is average absolute temperature, t is Student's test. At confidence level 95% and number of experimental points n≥20 Student's test $t \leq 2$.

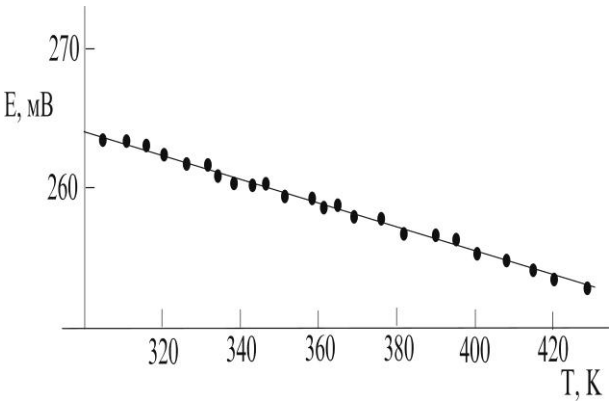

Fig. Temperature dependence of EFM chains of (5.16) type for melts of GdTe-Gd_2Te_3 subsystem.

Table

The results of computer treatment of EFM measurement results for the samples with compositions 51 and 55 at.% of Gd-Te system

T_i, K	E_i, мВ	$T_i-\overline{T}$	$E_i(T_i-\overline{T})$	$(T_i-\overline{T})^2$	$\tilde{\tilde{E}}$	$E_i-\tilde{\tilde{E}}$	$(E_i-\tilde{\tilde{E}})^2$
305,6	964,2	-56,90	-54862,98	3237,61	964,25	-0,05	0,00
311,2	963,8	-51,30	-49442,94	2631,69	963,75	0,05	0,00
316,3	963,4	-46,20	-44509,08	2134,44	963,29	0,11	0,01
321,9	963	-40,60	-39097,80	1648,36	962,79	0,21	0,04
327,2	962,6	-35,30	-33979,78	1246,09	962,32	0,28	0,08
332,3	962,3	-30,20	-29061,46	912,04	961,86	0,44	0,19
334,6	961,8	-27,90	-26834,22	778,41	961,66	0,14	0,02
338,4	961,4	-24,10	-23169,74	580,81	961,32	0,08	0,01
343,9	961	-18,60	-17874,60	345,96	960,83	0,17	0,03
347,7	960,2	-14,80	-14210,96	219,04	960,49	-0,29	0,08
351,2	960,7	-11,30	-10855,91	127,69	960,18	0,52	0,27
358,5	959	-4,00	-3836,00	16,00	959,53	-0,53	0,28
361,9	958,1	-0,60	-574,86	0,36	959,22	-1,12	1,26
365,2	958,5	2,70	2587,95	7,29	958,93	-0,43	0,18
369,1	958,1	6,60	6323,46	43,56	958,58	-0,48	0,23
376,3	957,1	13,80	13207,98	190,44	957,94	-0,84	0,71
381,1	957,2	18,60	17803,92	345,96	957,51	-0,31	0,10
390,7	956,7	28,20	26978,94	795,24	956,66	0,04	0,00
395,8	956,7	33,30	31858,11	1108,89	956,20	0,50	0,25
401,4	956,1	38,90	37192,29	1513,21	955,70	0,40	0,16
408,2	955,9	45,70	43684,63	2088,49	955,10	0,80	0,65
415,2	955,8	52,70	50370,66	2777,29	954,47	1,33	1,77
420,6	955,8	58,10	55531,98	3375,61	953,99	1,81	3,28
425,7	950,7	63,20	60084,24	3994,24	953,53	-2,83	8,03
$\overline{T}$ = 362,5	$\overline{E}$ = 959,17		$\sum E(T_i-\overline{T})$ =-2686,17	$\sum(T_i-\overline{T})^2$ =30118,72			$\sum(E_i-\tilde{\tilde{E}})^2$ =17,64

From the obtained equation

$$E, мВ = 991{,}5 - 0{,}089T \pm 2\left[\frac{0{,}80}{24} + 2{,}6\cdot10^{-5}(T-362{,}5)^2\right]^{1/2} \quad (2)$$

the relative partial thermodynamic functions of Gd in GdTe are calculated by known thermodynamic expressions:

$$\Delta\overline{G}_{Gd} = -279{,}3 \pm 0{,}3 \text{ kJ/mol} \quad (3)$$

$$\Delta\overline{H}_{Gd} = -287{,}3 \pm 1{,}6 \text{ kJ/mol} \quad (4)$$

$$\Delta\overline{S}_{Gd} = -26{,}7 \pm 4{,}3 \text{ J/(mol·K)} \quad (5)$$

These partial molar values are thermodynamic functions of potential forming reaction [8]:

$$Gd(sol.)+Gd_2Te_3(sol.)=3GdTe(sol.)$$

According to this reaction the standard thermodynamic formation functions GdTe can be calculated by ratios:

$$\Delta_f Z^0(GdTe) = \frac{1}{3}\left[\overline{\Delta Z}_{Gd} + \Delta_f Z^0(Gd_2Te_3)\right] \quad (6)$$

(Z≡G,H) and standard entropy by ratio:

$$S^0(GdTe) = \frac{1}{3}\left[\overline{\Delta S}_{Gd} + S^0(Gd) + S^0(Gd_2Te_3)\right] \quad (7)$$

According to these reactions the information by standard thermodynamic formation functions, standard entropy Gd_2Te_3 and also standard entropy of elementary gadolinium.

The standard free Gibb's energy of Gd_2Te_3 formation is calculated and the coherent complex of thermodynamic data for this compound:

$$\Delta_f G^0(298K) = -930{,}6 \pm 25{,}9 \text{ kJ/mol}$$

$$\Delta_f H^0(298K) = -926{,}3 \pm 22{,}2 \text{ kJ/mol}$$

$$S^0(298K) = 298{,}9 \pm 8{,}4 \text{ J/(mol·K)}$$

is obtained by us with the use of data [8] by standard heat of Gd_2Te_3 formation and also values of standard entropies of gadolinium (67,95±0,84 Дж·моль$^{-1}$·К$^{-1}$) and tellurium (49,50±0,21 Дж·моль$^{-1}$·К$^{-1}$) [7]. This compound is used at calculations by ratios (6) and (7).

In the result of calculations the following values of standard integral thermodynamic functions of GdTe are obtained:

$$\Delta_f G^0(298K) = -403{,}3 \pm 8{,}7 \text{ kJ/mol}$$

$$\Delta_f H^0(298K) = -404{,}4 \pm 7{,}9 \text{ kJ/mol}$$

$$S^0(298K) = 113{,}7 \pm 4{,}1 \text{ J/(mol·K)}$$

The errors are found by the method of mistake accumulation.

CONCLUSION

The system is investigated by rapid fixing method in two-phase region of GdTe+Gd_2Te_3 in temperature interval 300-430K. The relative partial molar functions of gadolinium in melts on the base of which the coherent complex of standard thermodynamic function of formation (ΔG^0_{298}, ΔH^0_{298}) and standard entropy of GdTe compound are firstly obtained.

[1] *E.I. Yarembash, A.A. Eliseev.* Xalkoqenidi redkozemelnix elementov. M.: Nauka, 1975. (In Russian).

[2] *O.V. Andreev, V.G. Bamburov, L.N. Monina, I.A. Razumkova, A.V. Ruseykina, O.Yu. Mitroshin, V.O. Andreev.* Fazovie ravnovesiya v sistemax sulfidov 3d-, 4f-elementov. Ekatirinburq: RIO URO RAN, 2015, 312s. (In Russian).

[3] *A.R. Jha*. Rare Earth Materials: Properties and Applications, CRC Press, United States, 2014.

[4] *N. Ru., Chu J.-H., and I.R. Fisher* Magnetic properties of the charge density wave compounds RTe_3 (R=Y, La, Ce, Pr, Nd, Sm, Gd, Tb, Dy, Ho, Er, and Tm). Phys. Rev. B 78, 2008, p.012410.

[5] *T.B. Massalski.* Binary alloys phase diagrams, second edition. ASM International, Materials park, Ohio, 1990, v.2, p.1163-1166.

[6] *O. Kubaschewski, C.B. Alcock.* P. J. Spenser Materials Thermochemistry. Pergamon Press, 1993, 350 p.

[7] *V.S. Yunqmana.* Baza dannix termicheskix constant veshestv. Elektronnaya versiya pod. red. 2006 q., http://www.chem.msu.su/cgi-bin/tkv (In Russian).

[8] *A.B. Agaev I K.A. Sharif.* Standarnaya entropiya obrazovaniya Gd_2Se_3 i Gd_2Te_3. Uchenie zapiski AGU, 1972, s. 72-74. (In Russian).

[9] *M.B. Babanli, Yu.A. Ysibov.* Elektroximicheskie metodi v termodinamike neorqanicheskix sistem. Baku. ELM. 2011. 306 s. (In Russian).

[10] *M.B. Babanli, S.Z. Imamalieva, G.I. Ibadova*. Vestnik BGU, seriya fiziko-matem. nauk, 2009, №4, s.5-9. (In Russian).

[11] *S.Z. Imamalieva, Z.S. Aliev, M.A. Maxmudova, M.B. Babanli, A.S. Abbasov.* Xim. Problemi, 2010, №3, s.453-456. (In Russian).

[12] *A.N. Kornilov, L.B. Stepina, B.A. Sokolov.* Jurn. fiz. ximii, 1972, t. 46, № 11, s. 2974-2979. (In Russian).

[13] *A.G. Morachevskiy, G.F. Voronin, V.A. Geyderix, I.B. Kuchenok*. Elektro-ximicheschekie metodi issledovaniya v termodinamike metallicheskix system ICK. «Akademkniqa», 2003, 334 s. (In Russian).

Recevied: 12.10.2017

DIELECTRIC RELAXATION OF HALOGENATED BENZENES IN MICRO-WAVE RANGE

S.T. AZIZOV, O.A. ALIYEV, K.E. ZULFUGARZADE
Institute of Physics of Azerbaijan National Academy of Sciences, H.Javid ave.,33, AZ 1143, Baku, Azerbaijan
e – mail: [1]samir_azizov@mail.ru

The complex dielectric constants of chlorbenzene, bromobenzene and iodobenzene at wave lengths 11,5cm and 12,8cm at temperatures from 20 up to - 80 ° C are measured. The jump appears in real and imaginary parts of complex dielectric constant in the point of phase transition in all investigated liquids. The temperature dependence of time of molecule dielectric relaxation in liquid state is found. It is revealed that increase of relaxation time takes place with increase of size halogen substituent. The thermodynamic values characterizing the dielectric relaxation process are calculated. The comparison of enthalpy of activation of dielectric relaxation processes is carried out.

Keywords: molecular spectroscopy, water dielectric properties, dielectric relaxation, benzene, chlorbenzene, bromobenzene, iodobenzene.
PACS: PACS: 30.00.00; 33.20. – t; 33.20.Bx

INTRODUCTION

The dielectric relaxation is observed in micro-wave range covering the part of electromagnetic wave spectrum by the length from 30cm up to 1mm in many polar liquids. The successful development of this range gives the premises for intensive investigation of relaxation properties. The interest to these liquids is explained by their comparative simple construction that allows us to use the existing theories for the analysis of experimental data. By data of works [1,2] there is some distribution of relaxation time decreasing with temperature increase in chlorbenzene and bromobenzene.

Later the presence of unique relaxation time is marked for the same compounds [3]. However, the high-frequency limit of ε_∞ Cole-Cole diagram is bigger than square of n^2 refraction index measured in infra-red range [4]. This fact is connected with probable existing of additional absorption region of resonance character in submillimeter range. Indeed, the explicit deviations from Debye properties of fluouro-, chlor-, bromo- and iodobenzene are found at wave lengths from 7 up to 3mm that is explained by the influence of rotational spectrum and it is noted that measurement accuracy is limited [5,6]. The overshoot of index absorption experimental value ε'' in comparison with its calculated value by low-frequency data in the case of chlorbenzene at wave length 3mm is explained as partial conferment of Poli's hypothesis. However, it is noted in work that chlorbenzene dielectric properties at λ=4,3mm can be calculated on the base of data obtained at longer waves [7]. These disagreements are explained by big experimental difficulties at work with very small wave lengths. In this connection the low-temperature measurement on longer waves is of a big interest.

Taking into consideration the strong dependence of second dispersion on temperature one can expect that such measurements give the some information on this phenomenon [8]. Besides, the low-temperature measurements allow us to reveal the some peculiarities of dielectric relaxation mechanism at the transition from liquid into solid state. Considering the halogenated benzenes the all works known from reference are carried out at temperatures higher than solidification point.

The temperature dependence of complex dielectric constant of chlorbenzene, bromobenzene and iodobenzene are studied by us. The temperature interval from 20 up to- 80°C is covered.

EXPERIMENTAL PART

The measurements are carried out in assembled installation working by principle of input resistance transformation of coaxial line filled by the investigated liquid in input of measuring line [9]. The shift of voltage node in measuring line significantly increases in comparison with usual method of short-circuit line in this method because of transformation that allows us to increase the measuring accuracy of ε^* strongly absorbing substances [10]. The cell with the sample is thermostated and cooling rate is **~0, 1** grad/min.

The inclination from average values for ε'don't exceed 1% and for ε''don't exceed 3%. The initial liquids are treated by drying under calcined chlorbenzene, bromobenzene and iodobenzene. After drying the liquids are rectified in rectifying column. The rectification is carried out three times.

The data of temperature dependence of complex dielectric constant $\varepsilon^* = \varepsilon' - i\varepsilon''$ of chlorbenzene, bromobenzene and iodobenzene are given in table 1. The data for chlorbenzene and iodobenzene are obtained at wave length 12,80cm and data for bromobenzene are obtained at wave length 11,50cm. The phase transition of all investigated substances coincides with jump of complex dielectric constant. Further the gradual increase of ε' real part up to value significantly exceeding the refraction index square and decrease of ε'' imaginary part up to zero take place in small temperature interval after jump.

The analogous jump of dielectric constant is observed at acoustic frequencies, in particular, in bromobenzene at frequency 400Hz whereas the losses are absent in whole temperature interval [11].

131 H.Javid ave, AZ-1143, Baku
ANAS, G.M.Abdullayev Institute of Physics
E-mail: jophphysics@gmail.com

Table 1

Complex dielectric constant $\varepsilon^* = \varepsilon' - i\varepsilon''$

	Chlorbenzene		Bromobenzene		Iodobenzene				Chlorbenzene		Bromobenzene		Iodobenzene	
t, ℃	ε'	ε''	ε'	ε''	ε'	ε''		t, ℃	ε'	ε''	ε'	ε''	ε'	ε''
Liquid state								Solid state						
20	5,60	0,54	5,17	0,82	4,38	0,67		- 31	–	–	3,05	0,38	–	–
10	5,72	0,65	5,22	0,93	4,35	0,75		- 32	–	–	3,03	0,22	3,06	0,42
0	5,83	0,78	5,31	1,09	4,27	0,84		- 35	–	–	2,93	0,16	2,98	0,22
-10	5,95	0,90	5,40	1,25	4,18	0,91		- 40	–	–	2,83	0,05	2,87	0,10
-20	6,07	1,09	5,31	1,41	4,08	0,97		- 46	3,18	0,30	2,82	–	2,85	0,03
-30	6,15	1,31	5,05	1,57	3,97	1,04		- 48	3,04	0,21	2,82	–	2,85	–
-40	6,16	1,51	–	–	–	–		- 50	2,96	0,17	2,82	–	2,85	–
-45	6,12	1,70	–	–	–	–		- 60	2,81	0,02	2,82	–	2,86	–
								- 70	2,80	–	2,83	–	2,85	–
								- 80	2,81	–	2,83	–	2,85	–

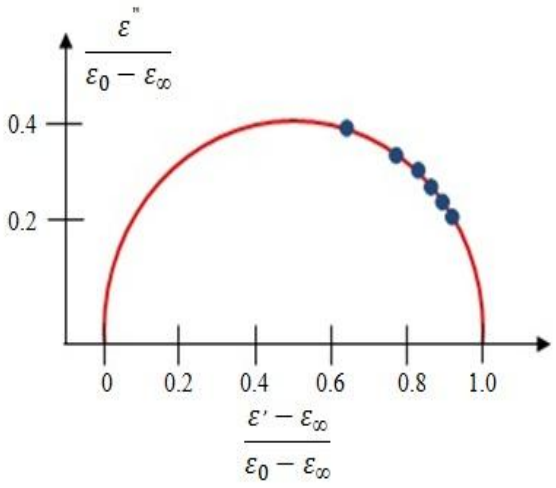

Fig. 1. The reduced diagram for bromobenzene (λ=11,50 cm).

From the table data it is seen that the peculiarities in temperature motion of complex dielectric constant

Taking into consideration data from table and notion about water structure one can conclude: the peculiarities in temperature dependence of complex dielectric constant connect with the presence of short-range order for water near solidification temperature that reveals itself in microformation form.

One can propose that molecules including in these microformations at temperature of solidification lose the freedom of rotating orientation whereas the rest molecules save it in some temperature interval below solidification point. It would be interesting to carry out the measurements in considered temperature region at more high frequencies where this transition probably reveals more clear.

The reduced diagram for bromobenzene is shown in fig.1. In the case of two other compounds the points are well marked in semicircle in abscissa axis.

This allows us to confirm that dielectric properties of all three liquids are totally successfully can be described with the help of one relaxation time up to the temperature of solidification. That's why the calculation of τ relaxation time is carried out by the formula:

$$\tau = \frac{1}{\omega}\,\frac{\varepsilon''}{\varepsilon' - \varepsilon_\infty} \qquad (1)$$

where ω is circular frequency of applied field. The relaxation time defined by formula (1) is the macroscopic one in the comparison from microscopic and molecular τ_μ relaxation times. The connection between them has the form $\tau = \gamma\tau_\mu$ where γ characterizes the inner field influence and depends on expression choice for the last one. Considering the inner field by Onsager we obtain the expression for γ:

$$\gamma = \frac{3\varepsilon_0}{2\varepsilon_0 + \varepsilon_\infty}. \qquad (2)$$

γ values calculated by formula (2) are given in first column of table 2. It is seen that practical γ value doesn't change with temperature and consequently, macroscopic and molecular relaxation times differ only by multiplicative constant. The knowing of temperature dependence of relaxation time gives the possibility to define the thermodynamic value characterizing the mechanism of dielectric relaxation process.

The consideration of polar molecular relaxation process as its transition from one equilibrium position into another one by the way of overcoming of energy barrier in theory of absolute velocities leads to the following expression:

$$\Delta F = 2{,}303\ RT\ lg\ (2{,}08\cdot 10^{10}\,\tau T), \qquad (3)$$

where ΔF is free activation energy.

Using the known thermodynamic ratio $\Delta F = \Delta H - T\Delta S$ and accepting ΔH activation enthalpy as constant one in considered temperature interval, its value can be defined from line inclination $\lg(\tau T) = \Phi(1/T)$ (fig. 2) by formula

$$\Delta H = 2{,}303\ R\frac{d(lg\tau T)}{d(1/T)}. \qquad (4)$$

The transition of activated molecule through energy barrier is accompanied by its bond breakage with neighbor molecules that is characterized by ΔH activation enthalpy value. As it is seen ΔF and ΔH increase with

increase of molecule size, moreover ΔH in all three cases is less than ΔF that leads to negative sign of ΔS activation entropy.

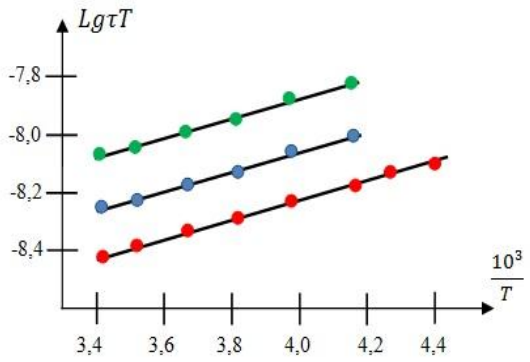

Fig. 2. Temperature dependence τT: *1(red)* is chlorbenzene, *2(blue)* is bromobenzene, *3(green)* is iodobenzene.

One can conclude that the phenomenon of dielectric polarization in studied liquids increases the degree of order in molecule disposition.

The additional information on dielectric relaxation can be obtained by the way of comparison of activation enthalpy value with corresponding data for viscous flow. From table 4 it is followed that ΔH_B activation enthalpy values defined from viscous measurements, exceed ΔH_D values for dielectric relaxation.

This can be quantitatively explained because of the fact that molecule makes the translation and rotational movements whereas it only rotates in dielectric relaxation process. However, as it is seen from table 4, the tendency to $\Delta H_B - \Delta H_D$ difference decrease is observed because of size increase of exchanging halogen. This probably shows the fact that the molecule rotational movement is also accompanied by translational movement with increase of its asymmetry.

Table 2

γ multiplier taking under consideration the inner field;
τ macroscopic and τ_μ molecular relaxation times ($\tau \cdot 10^{11}$ сек.)

τ,°C	Chlorbenzene			Bromobenzene			Iodobenzene		
	γ	τ	τ_μ	γ	τ	τ_μ	γ	τ	τ_μ
20	1,23	1,20	0,98	1,21	1,95	1,61	1,16	2,81	2,43
10	1,23	1,43	1,17	1,21	2,27	1,88	1,16	3,23	2,80
0	1,23	1,67	1,36	1,21	2,58	2,13	1,16	3,83	3,31
-10	1,24	1,86	1,50	1,22	2,85	2,35	1,16	4,45	3,85
-20	1,24	2,20	1,77	1,22	3,38	2,77	1,16	5,15	4,44
-30	1,25	2,61	2,10	1,22	4,22	3,45	1,17	6,05	5,20
-40	1,25	3,02	2,41	–	–	–	–	–	–
-45	1,25	3,44	2,75	–	–	–	–	–	–

Table 3

Activation enthalpy for ΔH_B viscous flow and dielectric relaxation ΔH_D *(kcal/mol)*

Substance	ΔH_B	ΔH_D	$\Delta H_B - \Delta H_D$
Chlorbenzene	1.61	1,49	0,12
Bromobenzene	1,72	1,65	0,07
Iodobenzene	1,82	1,79	0,03

ΔH values are given in table 3, values are given in table 3 and ΔF values are given in table 4.

Table 4

Free activation energy ΔF *(kcal/mol)*

τ,°C	ΔF		
	Chlorbenzene	Bromobenzene	Iodobenzene
20	2,50	2,79	3,00
10	2,49	2,74	2,95
0	2,47	2,71	2,93
-10	2,42	2,64	2,88
-20	2,39	2,61	2,82
-30	2,37	2,60	2,77
-40	2,31	–	–
-45	2,32	–	–

CONCLUSION

The complex dielectric constant of chlorbenzene, bromobenzene and iodobenzene at wave lengths 11,50 and 12,80cv in interval from 20 up to 80°C is measured.

The jump of real and imaginary parts of complex dielectric constant is observed for all investigated liquids in phase transition point. ε' decrease up to value significantly exceeding the refraction index square and ε'' decrease up to zero take place after jump in small temperature interval.

The temperature dependence of dielectric relaxation time for molecules in liquid state is defined.

The thermodynamic values characterizing the dielectric relaxation process are calculated. The comparison of activation enthalpy for processes of dielectric relaxation and viscous flow is carried out. The tendency to decrease of enthalpy difference for both processes is revealed with asymmetry increase.

[1] *K.E. Zulfugarzade, G.A. Gadjiev, L.M. Imanov.* Jurnal Fizicheskaya Ximiya, 1972, 46.
[2] *L.M. Imanov, K.E. Zulfiqarzade, L.A. Guliev.* Izvestiya AN Azerbaydjanskoy SSR, seriya FTMN, 1972, №5. (In Russian).
[3] *J.P h. Po1ey.* Appl. Sci. Res., 4 (5), 337, 1955.
[4] *K.S. Co1e, R.H. Co1e.* J. Chem. Phys., 9, 341, 1941.
[5] *B.G. Lone, P. Undre, S.S. Patil, P.W. Khirade and S.C. Mehrotra.* J. Mol. Liq., 141, 47 (2008).
[6] *Ch.O. Kadjar, S.T. Əzizov, O.A. Aliev, K.E. Zulfugarzade,.* Azerbaycan MEA Xəbərlər, Fizika, Riyaziyyat, Astronomiya, № 2, cild XXXIV, Bakı, 2015. (In Russian).
[7] *A. Chaudhari, A. Das, G. Raju, H. Chaudhari, P. Khirade, N. Narain, S.C. Mehrotra.* Proc. Natl. Sci. Counc. ROC (A) 25. 205, 2001
[8] *A. P. Maharolkar, A.G. Murugkar, S.S. Patil, P.W. Khirade.* "Characterization of Dominant Hydrogen Bonded Complex Structures", Asian Journal of Chemistry; Vol. 25, No. 2, 2013, 937-940
[9] *Ya.Yu. Axadov.* Dielektricheskie parametri; chistix jidkostey, Moskva, 1999, 854. (In Russian).
[10] *M. Lazarte, A.C. Gomez, Marigliano and H.N. Solimo.* J. Solut. Chem. 33, 1549, 2004.
[11] *A. Chaudhari, A.G. Shankarwar, B.R. Arbad, S.C. Mehrotra.* "Dielectric Relaxation in Glycine – Water and Glycine – Ethanol – Water Solutions Using Time Domain Reflectometry", Journal of Solution Chemistry, vol.33, № 3, March 2004, p. 313 – 322.

Recevied: 08.09.2017

METAL - $TlGaSe_2$ SEMICONDUCTOR - METAL STRUCTURE AS MEMRISTIVE SYSTEM

R.A. SULEYMANOV [1, 2, 3], MIR HASAN YU. SEYIDOV[1, 2] *, FAIK A. MIKAILZADE[1, 2], BUKET BILGEN KANDEMIR[1], YASIN ŞALE[1], TOFIG G. MAMMADOV[2]

[1]Department of Physics, Gebze Technical University, Gebze, Kocaeli 41400, Turkey
[2]Institute of Physics Azerbaijan National Academy of Sciences, AZ-1143 Baku, Azerbaijan
[3] Department of Electrical and Electronics Engineering, Antalya Bilim University, Antalya, Turkey
**Corresponding author. Address: Department of Physics, Gebze Technical University, Gebze, 41400, Kocaeli, Turkey. Tel.: +90 262 605 1329; fax: +90 262 653 8490*
E-mail address: smirhasan@gyte.edu.tr (M-H.Yu.Seyidov).

The influence of electric field and current flow on the current - voltage *(I – V)* characteristics of $TlGaSe_2$ layered semiconductor was investigated by using a two - point probe measurement system. Switching in *I – V* characteristics associated with memory effect was observed in all samples selected from different batches. Experimental findings were analyzed by using a model of metal – insulator – semiconductor – insulator – metal (MISIM) structure having memristive behavior.

Keywords: memristor; current – voltage characteristics; metal – insulator – semiconductor – insulator – metal structure; Lambert W – function.
PACS: 77.22.-d**;** 77.22. Ej; 77.70.+a; 77.80.-e

1. INTRODUCTION

Memristor is the fourth fundamental two - terminal passive circuit component in addition to resistor, capacitor and inductor. It first was postulated by Leon Chua in 1971 and proposed as the missing electronic component [1]. As the name suggests, memristor behaves similar to a conventional resistor, but it has a memory, in the sense that instantaneous resistance of memristor depends on its past values.

For several decades, different types of memristors have been developed as solid - state semiconductor devices, by using polymers, in plants, trees, fruits, biological tissues and so on. The semiconductor memrestive switching devices usually demonstrate rectifying type current - voltage characteristic. The underlying reason is that, the semiconductor forms a Schottky contact with one of the metallic electrodes and an ohmic contact with the other. In this configuration, reversible changes in *I - V* characteristics can be induced by applying a threshold electric field or bias current.

As it is well known, the switching can be unipolar or bipolar. In unipolar resistive switching, the switching direction depends only on the amplitude of the applied voltage or current, but not on the polarity, whereas in the case of bipolar resistive switching, an inversion of the polarity is required to switch back the *I - V* characteristics. In the sequel, we will focus only on the bipolar resistive switching, which is of special interest in an application perspective.

In experimental investigations, the memristive behavior is defined by specific *I – V* characteristics. Pinched hysteresis loop on the *I – V* characteristics in a shape of bow tie is considered as a distinctive property of memristive behavior. In this paper, we present diode - like *I - V* characteristics of Metal - $TlGaSe_2$ - Metal structure followed by switching effect registered by using a current controlled method, within the temperature range of 77 – 300 K. In order to control the polarity of the diode, we applied an electrical training process. This training process changes the polarization direction of Metal - $TlGaSe_2$ - Metal structure from forward to reverse, and hence switch the charge transport characteristics as well.

We will demonstrate that, the diode polarity rectification as well as sign of switching voltage depend on sweeping direction of the applied external current, i.e. from negative to positive values or vice versa. In other words, the resistance of the structure depends on the past states through which the system has evolved, which clearly suggests that the structure ***remembers*** the direction of current sweeping and demonstrates memristive behavior [1 - 4]. The investigated system is also characterized by the pinched hysteresis loops, which was observed in all samples worked with.

The memristive effect is due to the displacement of charge while applying a bias electric field. The strength of the electric field is proportional to the inverse square of the layer thickness within which the charges are mobile. Clearly, memristive effect is possible if the thickness of the active layer is in nanometer scale. In this paper, we demonstrate for the first time that memristive behavior is possible in bulk devices, which exhibit similar characteristics to their nanoscale counterparts.

The MISIM – memristor structures were built by using bulk $TlGaSe_2$ thin plates having two electrodes fabricated from different metals in planar and sandwich geometry of contacts. The accuracy of thin insulating layers on both surfaces of $TlGaSe_2$ samples is of key importance for this type of model. We also point out the existence of a nonzero imprinted electric field within the $TlGaSe_2$ sample following electrical poling, which is considered as a key factor for memristive behavior. Thin insulating layer near the surface of the semiconductor could be polarized under applied electric field due to migration of some charged entities such as ions in oxide materials, thus resulting in memristive behavior.

131 H.Javid ave, AZ-13, Baku
ANAS, G.M.Abdullayev Institute of Physics
E-mail: jophphysics@gmail.com

The effect of polarization on the overall structure will depend greatly on the resistance of the $TlGaSe_2$ sample, which can change substantially depending on temperature, thus changing the distribution of voltage drop between insulating film and semiconductor. At low temperatures, when the resistance of semiconductor is sufficiently high, $> 10^8\ \Omega$, the system will behave as an ohmic resistor with additional voltage superimposed on the applied one. At room temperatures ~ 300 K the resistivity of semiconductor decreases substantially to ~ $10^6\ \Omega$, and almost all applied voltage drops on the insulating layer. This mechanism provides diode behavior with controllable direction of rectification to the system.

We have obtained an analytical expression for *I - V* curves using Lambert W - function. This expression has been fitted to experimental data in order to obtain parameters of the electrically modelled diode circuit with a current source and series resistance.

2. EXPERIMENTAL PROCEDURE

For the Metal - $TlGaSe_2$ - Metal structure fabrication, initially undoped $TlGaSe_2$ single crystals grown by the modified Bridgman - Stockberger technology were used. $TlGaSe_2$ samples were picked from different batches. Their electrical resistivity was measured in dark, and was found to be larger than $10^6\ \Omega \cdot cm$ at ~ 300 K.

Different pairs of *Au*, *In,* and *Cu* - metallic contacts were prepared by evaporation on both sides of the freshly cleaved surfaces of the samples and were used to measure the conductivity along both directions, namely, parallel and perpendicular to the plane of layers. The measurements were performed by using three different $TlGaSe_2$ bulk samples, all having thicknesses around ~ 500 μm. The distance between the electrodes which were used for measuring the current in the direction parallel to the layers was ~ 2 mm. Samples were labeled and referred below as *F*, *Y*, and *Kh*. For example, *F Au - In* parallel refers to $TlGaSe_2$ sample from *F* - technological batch with the *Au* and *In* contacts deposited onto the top surface of the sample.

Samples were mounted on a cold finger and placed inside a Janis closed cycle helium cryostat. A control sensor (diode DT - 470) and a resistive control heater were mounted under the base and used to control the temperature by using a Lake Shore - 340 auto tuning temperature controller. Temperature of the samples was controlled within ~ 0.1 K accuracy by using a digital PID temperature controller.

I - V measurements were performed on three various structures fabricated from different $TlGaSe_2$ samples. Different pair of metallic electrodes of ~ 1.5 mm in diameter and about 100 nm in thickness were deposited on top and bottom layers of samples by thermal evaporation through a metal shadow mask. Electrical parameters were measured by using a two - probe method and a Keithley - 4200 semiconductor characterization system. *I - V* characteristics were registered at two different temperatures (300 and 140 K) in vacuum. The voltage bias was defined as positive when positive potential was applied to the *Au* electrode while the other electrode was connected to ground.

3. RESULTS

Typical *I - V* curves of all fabricated structures in a linear scale are shown in Fig. 1 (a - f). To study the resistance behaviors, the voltage bias was swept from – 40 V to + 40 V in both directions (indicated in Fig. 1 by arrows) and applied to the fabricated devices both at 300 and 140 K. Fig. 1 highlights that the resistance switching memory phenomenon can be observed during performing one cycle current sweep at room temperature. A high resistance state at 300 K is well maintained (cf. Fig. 1 (d - f)) when the positive current is increasing and until it reaches the set value. If current exceeds the set value, it dramatically increases, which puts the device in a low resistance state. The low resistance state can also be achieved by reversing the polarity of sweeping current, as depicted in Fig. 1 (a - c). It is easy to clarify that a resistance switching effect with memory during current sweep is not the only discernible peculiarity in Metal - $TlGaSe_2$ - Metal structure.

As it is seen from Fig. 1 all *I - V* curves registered at low temperature (140 K) are quasi - ohmic and highly asymmetric during forward and reverse biases at high temperature (300 K). Rectifying type current - voltage characteristics at room temperature was also observed for all samples independent of contacts and direction of current flow. As already mentioned above, the forward bias is defined as a positive ***dc*** voltage applied to the *Au* – electrode.

As illustrated in Fig. 1 (a - c), the *I - V* characteristics of fabricated structures registered at 300 K by sweeping current from positive to negative (as illustrated in Fig. 1 (a - c) by red arrows) demonstrate the rectifying behavior and resistance switching in the reverse bias region. Similarly, diode characteristics were observed by applying current from negative to positive with opposite rectification direction. In this case, resistance switching appears in the forward bias region, as shown in Fig.1 (d - f).

Another important effect was observed in the semi - logarithmic current – voltage curves shown in Fig. 1. Fig. 2 (a - b) demonstrates similar graphs, registered at different temperatures for *F Au - In* parallel $TlGaSe_2$ sample. Besides, the effects described above, which are correlated with the residual voltage, are clearly identified, especially at lower temperatures. The value and sign of this residual voltage as well as its temperature dependence can be clearly traced by the position of a “beak” corresponding to the voltage where current changes its sign. The sign of this voltage correlates with the sign of rectification, and temperature dependence of a “beak” shown in Fig. 2 (c) resembles the temperature dependence of conductivity of $TlGaSe_2$ crystals including non - monotonous behavior at low temperature range $T < 160$ K [5].

Described results clearly suggest that fabricated devices remember the direction of current sweeping or in other words the past states through which the system has evolved. Such behavior is characteristics of memristive systems [1].

It is well known that pinched hysteresis loop is a fingerprint of memristive behavior. Such behavior is demonstrated in Fig. 3 (a - c) for three different samples

hiving different contacts, and in different directions of current flow parallel and perpendicular to the plane of layers. As it is seen from Fig. 3, starting, say, from 30 V and going towards 0 V a relatively high current is observed (ON - state); however, situation changes drastically if the polarity of the applied voltage is changed: resistance substantially increases (OFF - sate) and then sample switches into the ON - state again. Returning back from the ON – state, current demonstrates the similar behavior: now the OFF - state as well as subsequent switching is observed at positive voltages. Thus, the loop locks.

4. DISCUSSION

The following questions arise after the findings described above: a) why I - V characteristic is ohmic at low temperatures and diode type at higher temperatures?; b) what is the mechanism of rectification in these $TlGaSe_2$ devices?; c) why the direction of rectification depends on the direction of current sweep?; d) what is the nature of residual voltage observed during current sweep?; e) what is the physical mechanism of switching in $TlGaSe_2$ crystals?

We start our discussion from the questions a) and b), that is, from the different character of I - V characteristic at low (140 K) and high (300 K) temperatures. In order to find answers to these questions, one must explain the nearly ohmic behavior at low temperature and diode type behavior at high temperature. Below we will show that different types of I - V characteristics at low and high temperature can be explained based on the diode model having a high series resistance. The current - voltage characteristics of fabricated structures is modelled by using the Lambert W – function [7].

In brief, the Lambert W - function, $W(x)$, is defined as the solution to the following transcendental equation: $yexp(y) = x$ [7]. In this investigation, we present for the first time an analytical solution for $TlGaSe_2$ - diode circuit model, which is based on the Lambert W – function. According to this model, I - V characteristic of fabricated devices can be described by following equation:

$$I = (qI_0R_s/kT) \cdot W\left[(qI_0R_s/kT) \cdot exp\left(q(V + I_0R_s)\right)/kT\right], \quad (1)$$

where k, q, and T are the Boltzmann constant, electron's charge and temperature, respectively. R_s is the series resistance, V – is voltage and I_0 – is the diode reverse current. Taking I_0 and R_s as fitting parameters, I - V dependences of fabricate devices were calculated. Results are shown in Fig. 4 (b). Calculations give the ohmic behavior at 140 K and rectified diode - type behavior at 300 K.

The physical explanation of this effect is rather simple. The $TlGaSe_2$ crystal is considered as a semiconductor material with presence of thin or ultrathin insulated layers at the semiconductor - metal interfaces. As a rule, the value of active resistance of the semiconductor is always in series with the electrical resistance of the metal - semiconductor contacts. Semiconductor electrical resistance can significantly change under certain circumstances, such as temperature, external pressure or radiation absorption.

At low temperatures, when series resistance is very high, $>10^8$ Ω, approximately all voltage drops on the series resistance, which leads to an ohmic characteristic. At higher temperatures, when series resistance decreases by two order of magnitude, approximately all voltage drops on the barrier at the semiconductor - metal interfaces and diode type I - V characteristic is registered.

Apparently, the role of series resistance in Metal - $TlGaSe_2$ - Metal structure plays $TlGaSe_2$ semiconductor crystal. What is the mechanism of diode - type rectification of this device? To some extent, it is really a ***strange*** diode, as its rectification direction depends on the polarity of the applied voltage, independent of the contact materials.

For example, considering $\boldsymbol{p}$ - type conductivity of $TlGaSe_2$, upon starting an I - V measurement, if negative voltage is applied to the Au contact, this contact acts as a blocking contact. On the other hand, if positive voltage is applied to the same contact upon starting I - V measurement, it acts as an ohmic contact, (see Figs. 1 and 2). Therefore, one can use an electrical training process to control the polarity of this diode. This further suggests that, by changing the polarization direction of the external bias, one can switch the transport characteristics between forward and reverse diodes.

The blocking character of metal – $\boldsymbol{p}$ - semiconductor junction means that due to electron interchange between the metal and semiconductor, depletion region occurs near the metal semiconductor boundary with the electrical field directed from metal towards semiconductor. Thus, another contact must acts as an ohmic contact. It was shown in a number of our recent studies [9 - 11] that, the voltage applied to the metallic contact creates an intrinsic electric field near the surface of $TlGaSe_2$ samples. The direction of this field depends on the polarity of applied voltage, where it always opposes to the direction of applied electric field. In other words, independent of the contact material, it may acts as a blocking or ohmic contact. In order to explain such effect, we proposed the model of native thin insulating layer on the surface of $TlGaSe_2$ crystal [11]. The electric field created near the contact is due to polarization of the native insulating layer on the surface of the crystal. Independent of the mechanism of such polarization, we may conclude that considering the current flow in $TlGaSe_2$ semiconductor one must take into account that in a $\boldsymbol{p}$ – semiconductor, both holes and some charged entities are forced to move simultaneously while an external voltage is applied to the system. This ıs similar to the discussion in [2], which describes the first realization of memristive behavior in Pt - TiO_2 - Pt system.

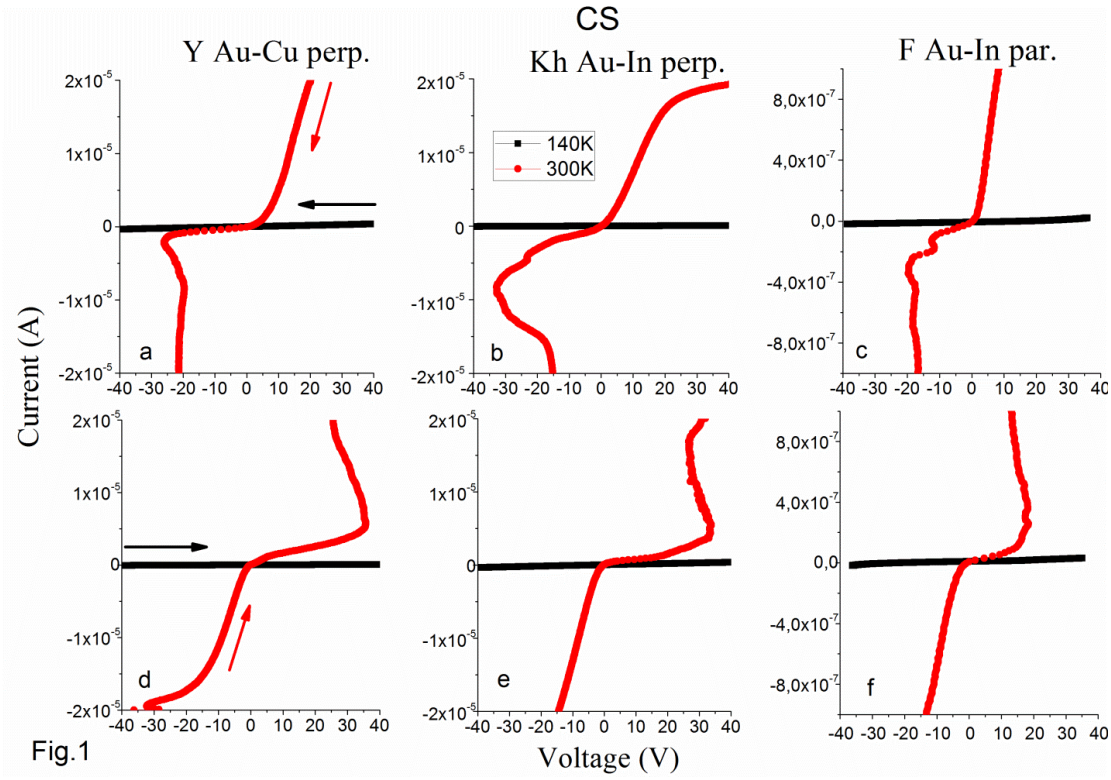

Fig. 1. I - V characteristics of different $TlGaSe_2$ samples measured by current sweep method in linear scale at two different temperatures; 140 and 300 K. Arrows indicate the direction of sweep.

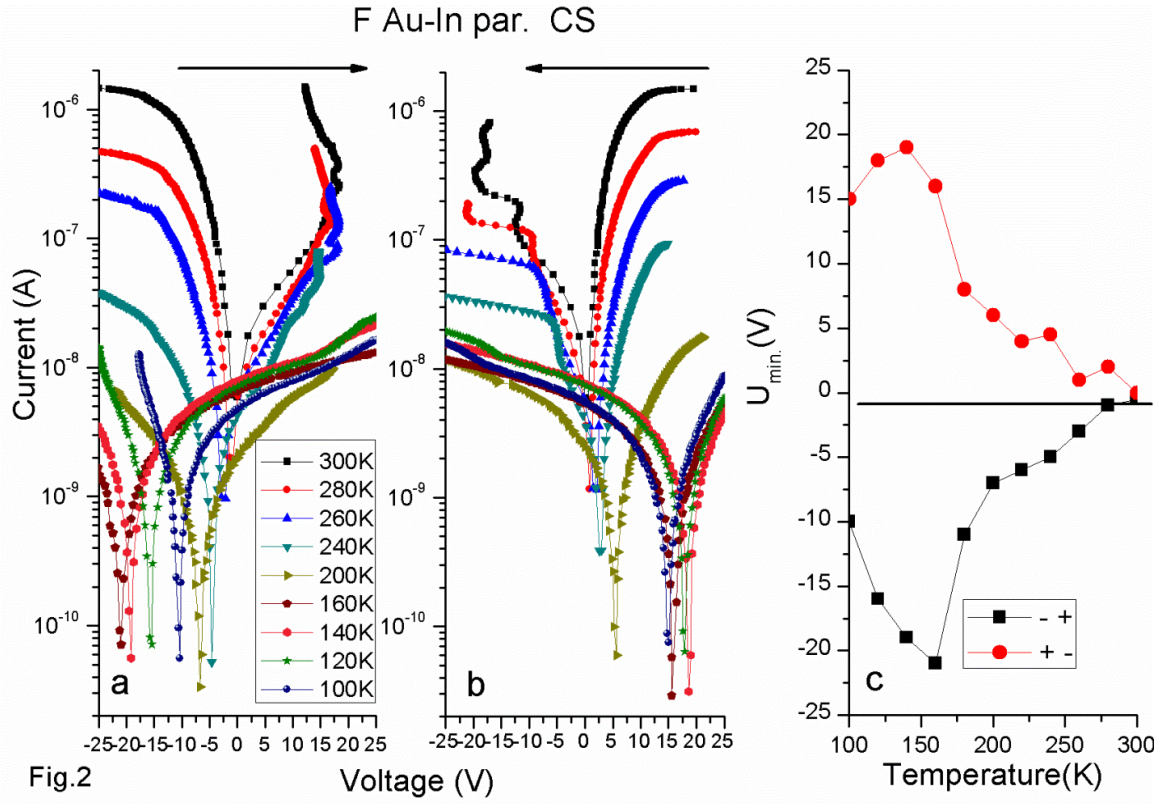

Fig. 2. a) and b) *I - V* characteristics of *F* – type $TlGaSe_2$ sample with *Au - In* metallic electrodes deposited on the top surface of crystal parallel to the layers. The measurements were carry out in current sweep method. *I - V* characteristics are displayed in logarithmic scale and corresponded to different temperatures. Arrows indicate the direction of sweep; c) The temperature dependences of "beak" position in Fig. 2 (a and b) for different direction of sweep.

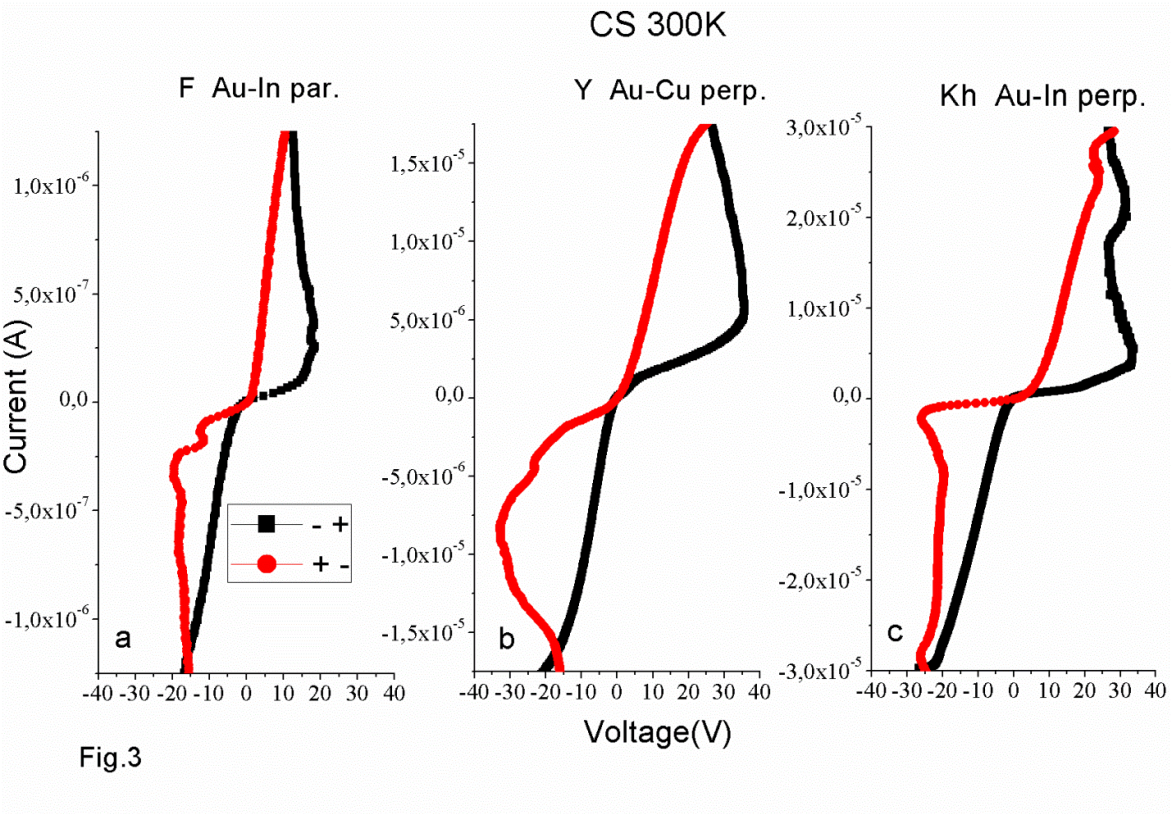

Fig. 3. The Pinched hysteresis loops registered for three different $TlGaSe_2$ samples by current sweep method at 300 K.

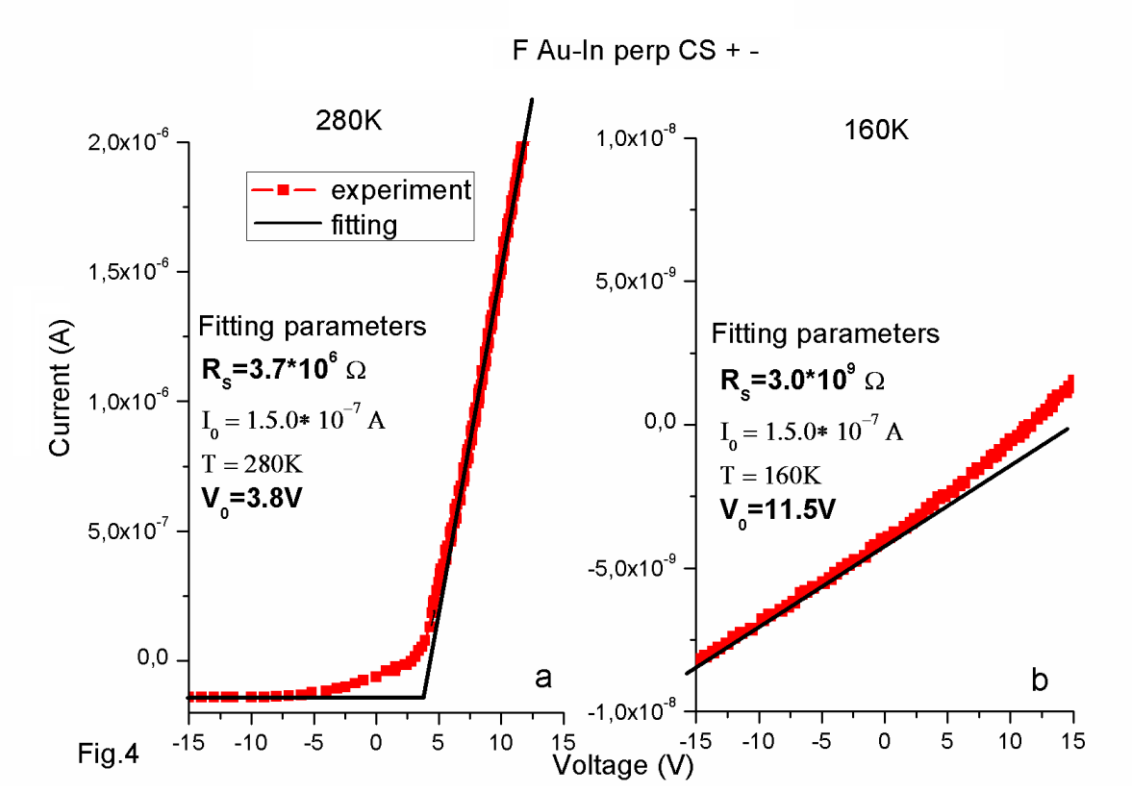

Fig.4. a) Experimental *I - V* characteristics of *Kh* - type $TlGaSe_2$ sample with *Au - In* metallic electrodes deposited on the top and bottom surfaces of crystal perpendicular to the layers. The measurements were carry out in current sweep method. *I - V* characteristics are displayed in linear scale at two different temperatures; 140 and 300 K. Sweep direction is from negative to positive values; b) – Results of fitting based on the diode model with series resistance. Calculations were made using formula (1). Fitting parameters are shown in figure.

Unlike our situation, it was established in [2,3] that charged entities mentioned above are charged oxygen vacancies which act above all as dopants. Moreover, it was shown in [11] that Pt - TiO_2 - Pt system behaves as a

Currently, we cannot claim whether or not the mechanism of charged ions migration within the electric field that is known in oxides [12 - 15] is applicable to native thin insulating layer proposed on the surface of $TlGaSe_2$ crystal. However, we can definitely state that, the observed memristive behavior in Metal - $TlGaSe_2$ - Metal structure is related with the migration of some mobile charged entities under the applied electric field. Such a model, which takes the memristive behavior of the investigated structure into account, makes the switching

5. CONCLUSIONS

In summary, we proposed the following model for the Metal - $TlGaSe_2$ - Metal structure: native thin insulating layer exists near the semiconductor surface, which can be polarized by applying an external electric field, due to migration of some charged entities such as ions in oxide materials. This layer provides the memristive behavior to this structure. The effect of such polarization on the overall structure will depend greatly on the resistance of the sample which can change

rectifier with controllable direction of rectification due to the electrical control of the chemical states in TiO_2-x such as the oxygen vacancy concentration at the interfaces between the TiO_2-x layer and Pt - electrodes.

phenomena quite understandable as well. As it is outlined in Chua's work [16]: all two - terminal non - volatile memory devices based on resistance switching are memristors, regardless of the device material and mechanism of operation. Apparently, the opposite proposition has also become true, because in the last decade, significant progresses has been made in understanding the resistive switching mechanisms based on the memristive type behavior independent of exact memory mechanism [17].

substantially with respect to temperature; thus changing the distribution of voltage drop between insulating film and semiconductor. At lower temperatures, when the resistance of semiconductor is sufficiently high, $> 10^8$ Ω, the system will acts as an ohmic resistor with additional voltage superimposed on the applied one, (see Fig.2). At higher temperatures close to 300 K the resistivity of semiconductor decreases substantially, 10^6 Ω, and almost all applied voltage drops on the insulating layer thus providing diode behavior to the system with controllable direction of rectification.

[1] *L. Chua.* Appl. Phys. A 102, 765 (2011).

[2] *Ronald Tetzlaff (ed.).* Memristors and Memristive Systems (Springer, New York, Heidelberg, Dordrecht, London 2014).

[3] *D.B. Strukov, G.S. Snider, D.R. Stewart, and R.S. Williams,* Nat. Lett. 453, 80 (2008).

[4] *Yuriy V. Pershin and Massimiliano Di Ventra.* Advances in Physics 60, 145 (2011).

[5] *Ferid Salehli, Yakup Bakıs, MirHasan Yu. Seyidov, and Rauf A Suleymanov.* Semicond. Sci. Technol. 22, 843 (2007)

[6] *MirHasan Yu. Seyidov, R. A. Suleymanov, Ertan Balaban, and Y. Şale.* Solid - State Electronics 94, 39 (2014)

[7] *Adelmo Ortiz-Conde, Francisco J. Garcia Sanchez, Juan Muci.* Solid - State Electronics 44, 1861 (2000).

[8] *MirHasan Yu. Seyidov, R. A. Suleymanov, Ertan Balaban, and Y. Şale.* J. Appl. Phys.114, 093706 (2013).

[9] *MirHasan Yu. Seyidov, R. A. Suleymanov, Ertan Balaban, and Y. Şale.* J. Appl. Phys.116, 213702 (2014).

[10] *MirHasan Yu. Seyidov, R. A. Suleymanov, Ertan Balaban, and Y. Şale.* Appl. Phys. Lett 105, 152106 (2014).

[11] *Hisashi Shima, Ni Zhong and Hiro Akinaga.* Appl. Phys. Lett. 94, 082905 (2009).

[12] *J. R. Jameson, Y. Fukuzumi, Z. Wang, P. Griffin, K. Tsunoda, G. I. Meijer, and Y. Nishi.* Appl. Phys. Lett. 91, 112101 (2007).

[13] *R. Waser and M. Aono.* Nat. Mater. 6, 833 (2007).

[14] *Y. Yang and W. Lu.* Nanoscale 5, 10076 (2013).

[15] *D.S. Jeong, H. Schroeder, and R. Waser.* Phys. Rev. B 79, 195317 (2009).

[16] *Leon Chua.* Appl. Phys. A 102, 765 (2011)

[17] *Yuchao Yang and Wei Lu.* Nanoscale, 5, 10076 (2013).

Recevied: 20.11.2017

ISSN 1028-8546

2017, Vol. XXIII, № 4
Section: En

CONTENTS